Specific Synthesis and Reaction of Hetero- and Homobridged Diruthenium Carbonyl Complexes Containing One or Two μ -Azolato Bridges

Kom-Bei Shiu,* Wei-Ming Lee, and Chen-Lan Wang

Department of Chemistry, National Cheng Kung University, Tainan, Taiwan 701, Republic of China

Sue-Lein Wang and Fen-Ling Liao

Department of Chemistry, National Tsing Hua University, Hsinchu, Taiwan 300, Republic of China

Ju-Chun Wang and Lin-Shu Liou

Department of Chemistry, Soochow University, Taipei, Taiwan 111, Republic of China

Shie-Ming Peng and Gene-Hsiang Lee

Department of Chemistry, National Taiwan University, Taipei, Taiwan 106, Republic of China

Michael Y. Chiang

Department of Chemistry, National Sun Yat-Sen University, Kaohsiung, Taiwan 804, Republic of China

Received February 5, 1996[⊗]

Diruthenium(I) carbonyl complexes with either hetero- or homobridges, [Ru₂(\mu-Pz)₂(CO)₄- $(HPz)_2$ (1), $[Ru_2(\mu-Pz')(\mu-O_2CMe)(CO)_4(HPz')_2]$ (2), and $[Ru_2(\mu-Pz')_2(CO)_4(HPz')_2]$ (3), can be prepared specifically. These complexes reacted with either nucleophiles or electrophiles to produce selectively only one product. The terminal azole groups, pyrazole (HPz) or 3,5dimethylpyrazole (HPz'), of 1-3 are easily replaced by the phosphine ligands to give [Ru₂- $(\mu - Pz)_2(CO)_4(PPh_3)_2$] (4), $[Ru_2(\mu - Pz')(\mu - O_2CMe)(CO)_4(PPh_3)_2]$ (5), $[Ru_2(\mu - Pz')_2(CO)_4(PPh_3)_2]$ (6), and $[Ru_2(\mu-Pz)_2(CO)_4(\eta^1-dppm)_2]$ (7). The μ -acetato bridge is more fragile than the μ -azolato bridge, and only the former bridge of 5 can be replaced by Pz⁻ and SR⁻ to afford [Ru₂(μ - $Pz'(\mu-Pz)(CO)_4(PPh_3)_2$ (8) and $[Ru_2(\mu-Pz')(\mu-SR)(CO)_4(PPh_3)_2]$ (R = Ph (9), tBu (10)). Heating the mixture of **3** with dppm in THF gave a product retaining all the μ -azolato bridges but losing two carbonyls, $[Ru_2(\mu-Pz')_2(CO)_2(\mu_1,\eta^2-dppm)_2]$ (11), whereas a similar reaction between 1-3 and nitrogen-bidentate ligands gave products retaining all four carbonyls but only one μ -azolato bridge, $[Ru_2(\mu-L)(\mu-CO)_2(CO)_2(\mu_1,\eta^2-(N-N))_2]^+$ (L = Pz, N-N = bpy ([12]+), phen ([13]⁺); L = Pz', N-N = bpy ([14]⁺), phen ([15]⁺)). The electrophilic addition of 4 with I_2 produced [Ru₂(*u*-Pz)₂(*u*-I)(CO)₄(PPh₃)₂][I₃] (**16**). The X-ray structure of this product confirms the cleavage of the Ru–Ru bond rather than the μ -azolato bridges. However, the μ -azolato and -acetato bridges, as well as the terminal azole groups, of **1–6** can be easily removed by an electrophilc reagent such as Et₃O+BF₄⁻ in the presence of MeCN to give [Ru₂(CO)₄- $(MeCN)_6][BF_4]_2$ and $[Ru_2(CO)_4(MeCN)_4(PPh_3)_2][BF_4]_2$.

Introduction

The coordination chemistry of the dirhodium and -iridium complexes has been well studied recently. Particularly, those containing the $\mu\text{-azolato}$ bridging group are under intensive investigations, due to the ability of the apparently strong $\mu\text{-azolato}$ bridge enabling to straddle an unusual range of intermetallic separations to hold two adjacent metal centers in chemically extremely stable configurations. 1 In view of the rarely studied coordination chemistry of the diruthenium complexes with the $\mu\text{-azolato}$ bridge, 2 and the significance of the diruthenium(I) carbonyl complexes

[®] Abstract published in Advance ACS Abstracts, May 15, 1996.

in being either involved as the active intermediates in homogeneously catalyzed reactions or catalytic precursors for the carbonylation of amines, the hydrogenation of carboxylic acids, and the addition of acetic acid to alkynes,³ we decided to explore the synthesis and reactivity some diruthenium(I) carbonyl complexes containing the μ -azolato linkage.

In this paper, we present the following new information: (1) a convenient approach to prepare *specifically* both hetero- and homobridged diruthenium carbonyl complexes with one or two μ -azolato linkages, (2) the *selective* nucleophilic and electrophilic reactions of these complexes to give only one type of product, (3) the X-ray

structures of eight representative reaction products, and (4) the novel propensity of the μ -azolato linkage, especially the cleavable feature first found in the dimetal system.

Results and Discussion

Synthesis. Although complexes $[Ru_2(\mu\text{-}L)_2(CO)_6]$ (HL = pyrazole (HPz), 3,5-dimethylpyrazole (HPz')) were previously described to be important precursors to several other ruthenium derivatives, the synthetic approaches used suffer either a low yield^{2a,e} or a tedious procedure. As demonstrated below, new dinuclear species in the types of $[Ru_2(\mu\text{-}L)_2(CO)_4(HL)_2]$ and $[Ru_2(\mu\text{-}Pz')(\mu\text{-}O_2CMe)(CO)_4(HPz')_2]$ can be obtained specifically in satisfactory yield and employed as better precursors to a variety of other Ru(I) and Ru(II) derivatives. Importantly, all the conversions appear to follow selective pathways.

In the presence of Et_3N , *catena*- $[Ru(O_2CMe)(CO)_2]$ reacted with excess HPz or HPz' in EtOH gave only one diruthenium derivative with either homo- or heterobridges, $[Ru_2(\mu-Pz)_2(CO)_4(HPz)_2]$ (1) and $[Ru_2(\mu-Pz')(\mu-Q_2CMe)(CO)_4(HPz')_2]$ (2), respectively. The homogridged compounds 1 can be obtained alternatively from the reaction of $[Ru_2(CO)_4(MeCN)_6][BF_4]_2$ with HPz/Et₃N and H₂O. Complex $[Ru_2(\mu-Pz')_2(CO)_4(HPz')_2]$ (3) can be

(1) (a) Uson, R.; Oro, L. A.; Ciriano, M. A.; Pinillos, M. T. *J. Grganomet. Chem.* **1981**, *205*, 247. (b) Beveridge, K. A.; Bushnell, G. M.; Dixon, K. R.; Eadie, D. T.; Stobart, S. R.; Atwood, J. L.; Zaworotko, M. J. *J. Am. Chem. Soc.* **1982**, *104*, 920. (c) Coleman, A. W.; Eadie, D. E.; Stobart, S. R.; Zaworotko, M. J.; Atwood, J. L. *J. Am. Chem. Soc.* **1982**, *104*, 922. (d) Bushnell, G. W.; Fjeldsted, O. K.; Stobart, S. R.; Zaworotko, M. J. *J. Chem. Soc., Chem. Commun.* **1983**, 580. (e) Beveridge, K. A.; Bushnell, G. W.; Stobart, S. R.; Atwood, J. L.; Zaworotko, M. J. *Organometallics*, **1983**, *2*, 1447. (f) Bushnell, G. W.; Stobart, S. R.; Vefghi, R.; Zaworotko, M. J. J. Chem. Soc., Chem. Soc., Chem. Commun. 1984, 282. (g) Atwood, J. L.; Beveridge, K. A.; Bushnell, G. W.; Dixon, K. R.; Eadie, D. T.; Stobart, S. R.; Zaworotko, M. J. Inorg. Chem. 1984, 23, 4050. (h) Bushnell, G. W.; Fjeldsted, D. O. K.; Stobart, R.; Zaworotko, M. J.; Knox, S. A. R.; Macpherson, K. A. Organome-allics 1985, 4, 1107. (i) Bushnell, G. W.; Decker, M. J.; Eadie, D. T.; Stobart, S. R.; Vefghi, R.; Atwood, J. L.; Zaworotko, M. J. Organometallics 1985, 4, 2106. (j) Claver, C.; Kalck, P.; Ridmy, M.; Thorez, A.; Gro, L. O.; Pinillos, M. T.; Apreda, M. C.; Cano, F. H.; Foces-Foces, C. J. Chem. Soc., Dalton Trans. 1988, 1523. (k) Caromna, D.; Oro, L. O.; Eerez, P. L.; Tiripicchio, A.; Tiripicchio-Camellini, M. *J. Chem. Soc., Palton Trans.* **1989**, 1427. (l) Pinillos, M. T.; Elduque, A.; Oro, L. A. *Frorg. Chim. Acta* **1990**, *178*, 179. (m) Pinillos, M. T.; Elduque, A.; Oro, 🖫 A.; Lahoz, F. J.; Bonati, F.; Tiripicchio, A.; Tiripicchio-Camellini, M. J. Chem. Soc., Dalton Trans. 1990, 989. (n) Pinillos, M. T.; Elduque, ; Lopez, J. A.; Lahoz, F. J.; Oro, L. A. J. Chem. Soc., Dalton Trans. 1991, 1391. (o) Carmona, D.; Ferrer, J.; Lahoz, F. J.; Oro, L. A.; Reyes, J.; Esteban, M. J. Chem. Soc., Dalton Trans. 1991, 2811. (p) Carmona, D.; Ferrer, J.; Mendoza, A.; Lahoz, F. J.; Reyes, J.; Oro, L. A. *Angew. Chem., Int. Ed. Engl.* **1991**, *30*, 1171. (q) Pinillos, M. T.; Elduque, A.; Oro, L. A. Polyhedron 1992, 11, 1007. (r) Ciriano, M. A.; Tena, M. A.; Oro, L. A. *J. Chem. Soc., Dalton Trans.* 1992, 2123. (s) Pinillos, M. T.; Elduque, A.; Lopez, J. A.; Lahoz, F. J.; Oro, L. A.; Mann, B. E. *J. Chem. Soc., Dalton Trans.* **1992**, 2389. (t) Tejel, C.; Ciriano, M. A.; Oro, L. A.; Tiripicchio, A.; Ugozzoli, F. Organometallics 1994, 13, 4153

(2) (a) Cabeza, J. A.; Landazuri, C.; Oro, L. A.; Tiripicchio, A.; Tiripicchio-Camellini, M. J. Organomet. Chem. 1987, 322, C16. (b) Sherlock, S. J.; Cowie, M.; Singleton, E.; Steyn, M. M. d. V. J. Organomet. Chem. 1989, 361, 353. (c) Neumann, F.; Süss-Fink, G. J. Organomet. Chem. 1989, 367, 175. (d) Neumann, F.; Stoeckli-Evans, H.; Süss-Fink, G. J. Organomet. Chem. 1989, 379, 151. (e) Cabeza, J. A.; Landazuri, C.; Oro, L. A.; Belletti, D.; Tiripicchio, A.; Tiripicchio-Camellini, M. J. Chem. Soc., Dalton Trans. 1989, 1093.

(3) (a) Bianchi, M.; Menchi, G.; Francalanci, F.; Piacenti, F.;

(3) (a) Bianchi, M.; Menchi, G.; Francalanci, F.; Piacenti, F.; Matteoli, U.; Frediani, P. J. Organomet. Chem. 1980, 188, 109. (b) Bianchi, M.; Iani, P. F.; Matteoli, U.; Menchi, G.; Piacenti, F.; Petrucci, G. J. Organomet. Chem. 1983, 259, 207. (c) Suss-Fink, G.; Hermann, G.; Morys, P.; Ellermann, J.; Veit, A. J. Organomet. Chem. 1985, 284, 263. (d) Matteoli, U.; Menchi, G.; Frediani, P.; Bianchi, M.; Piacenti, F. J. Organomet. Chem. 1985, 285, 281. (e) Kalck, P.; Sianti, M.; Jenck, J.; Peyrille, B.; Peres, Y. J. Mol. Catal. 1991, 67, 19. (f) Frediani, P.; Bianchi, M.; Salvini, A.; Guarducci, R.; Carluccio, L. C.; Piacenti, F. J. Organomet. Chem. 1995, 498, 187.

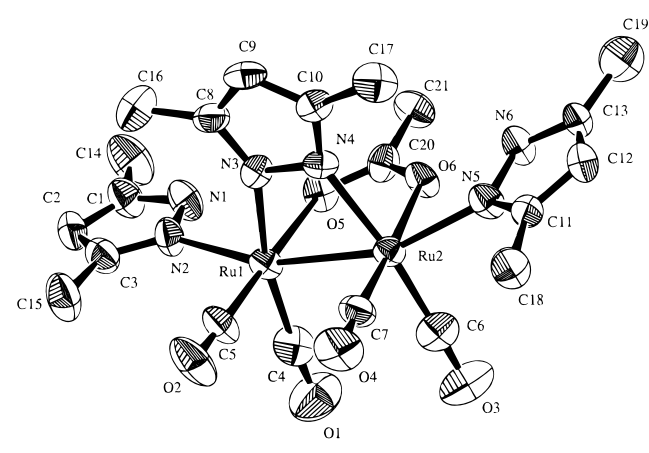
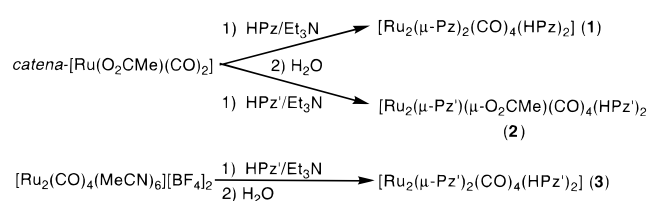


Figure 1. ORTEP plot of **2** with 50% thermal ellipsoids.

Scheme 1



obtained likewise. The reactions involve obviously first the substitution of MeCN in $[Ru_2(CO)_4(MeCN)_6][BF_4]_2$ with a better $\sigma\text{-donor},\,L^-,\,$ via HL/Et_3N to give $[Ru_2(\mu,\eta^2-L)_2(CO)_4(\eta^1-L)]^{2^-}$ and then protonation with H_2O to give 1 and 3 (Scheme 1). The specific formation of 2 rather than a mixture of 2 and 3 reflects probably that the nucleophilic substitution is stepwise and the steric hindrance of $\mu\text{-Pz}'$ in 2 may inhibit a subsequent replacement of the remaining $\mu\text{-acetato}$ group by a second Pz'^- .

Compound **2** was structurally characterized (Figure 1). The heterobridged feature and the two HPz' groups ligated to Ru at the axial sites were confirmed. The Ru–Ru distance of 2.682(1) Å in **2** (Table 1) is significantly shorter than that of 2.705(2) Å in $[Ru_2(\eta^2-Pz')_2-(CO)_6]^{2a,e}$. The longer distance may be due to a combination of both electronic and steric factors. The higher *trans* influence of the axial carbonyls in this compound, compared with that of the axial HPz' groups in **2**, and the larger nonbonded interactions between two bulky μ -Pz' groups and other groups in $[Ru_2(\eta^2-Pz')_2(CO)_6]$, compared with those between one such μ -Pz' group and other groups in **2**, may contribute to the Ru–Ru elongation

Reactions with Nucleophiles. The two axial groups in either $[Ru_2(\eta^2-L)_2(CO)_6]^{2e}$ or $[Ru_2(CO)_4(MeCN)_6]^{2+4a}$ were previously reported to be substitution labile. Complexes **1**–**3** behave similarly. The two axial HL groups of **1**–**3** are easily replaced by phosphine groups to give $[Ru_2(\mu-Pz)_2(CO)_4(PPh_3)_2]$ (**4**), $[Ru_2(\mu-Pz')(\mu-O_2-CMe)(CO)_4(PPh_3)_2]$ (**5**), $[Ru_2(\mu-Pz')_2(CO)_4(PPh_3)_2]$ (**6**), and $[Ru_2(\mu-Pz)_2(CO)_4(\eta^1-dppm)_2]$ (**7**) (Scheme 2) with **5** structurally characterized to confirm the heterobridged feature (Figure 2). The Ru–Ru distance increases from 2.682(1) Å in **2** to 2.7261(9) Å in **5**, apparently due to the increased nonbonded interactions between the bulkier PPh₃ groups and other groups in the molecule.

^{(4) (}a) Klemperer, W. G.; Zhong, B. *Inorg. Chem.* **1993**, *32*, 5821. (b) Shiu, K.-B.; Li, C.-H.; Chan, T.-J.; Peng, S.-M.; Cheng, M.-C.; Wang, S.-L.; Liao, F.-L.; Chiang, M. Y. *Organometallics* **1995**, *14*, 524.

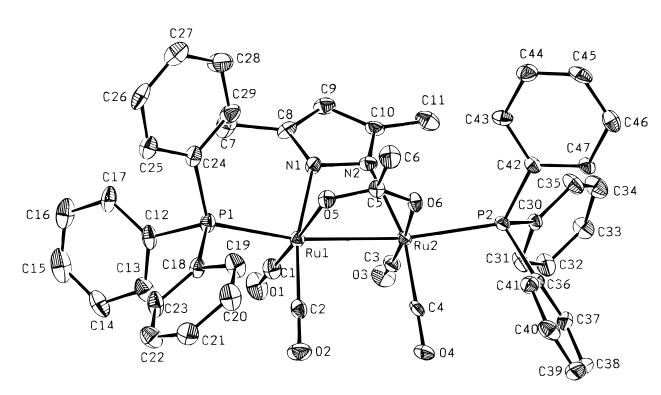
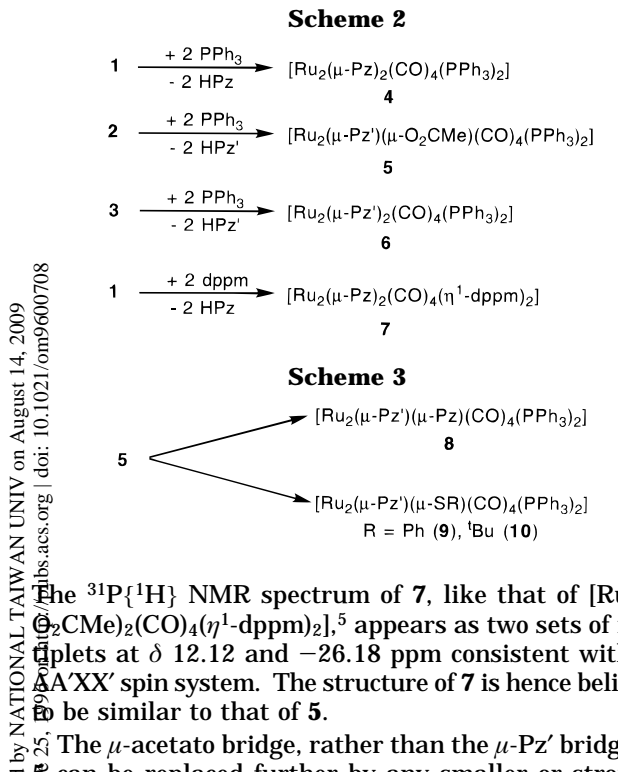


Figure 2. ORTEP plot of 5 with 50% probability ellipsoids.



The ${}^{31}P{}^{1}H}$ NMR spectrum of 7, like that of $[Ru_2(\mu \Theta_2$ CMe)₂(CO)₄(η^1 -dppm)₂],⁵ appears as two sets of multiplets at δ 12.12 and -26.18 ppm consistent with an AA'XX' spin system. The structure of 7 is hence believed

 \mathfrak{A} The *u*-acetato bridge, rather than the *u*-Pz' bridge, in **\\$** can be replaced further by any smaller or stronger **a**mionic σ -donor, like Pz⁻ or thiolate anion, to give [Ru₂- \mathcal{Q}_{μ} -Pz')(μ -Pz)(CO)₄(PPh₃)₂] (**8**) and [Ru₂(μ -Pz')(μ -SR)- $(CO)_4(PPh_3)_2$] (R = Ph (9), ^tBu (10)) (Scheme 3), respec-Evely. The ${}^{31}P{}^{1}H{}$ NMR spectrum of **10** appears as two doublets indicating probably the asymmetric orientation of either two PPh₃ groups and/or the thiolate bridge with respect to the Ru-Ru bond. 10 may be rigid in solution at room temperature on the NMR time scale. The single-crystal structure of **10** was thus carried out (Figure 3a). It reveals two asymmetrical PPh₃ groups (Figure 3b) with the P(2) group at the axial site and the P(1) group at the equatorial site, probably alleviating the repulsive nonbonded interactions if both groups are at the axial sites. The Ru-Ru distance is 2.7469(5) Å.

The reaction product between $[Ru_2(\mu-Pz')_2(CO)_6]$ and excess dppm was previously reported by Süss-Fink's group to be $[Ru_2(\mu-Pz')_2(CO)_4(\eta^1-dppm)_2]$, a formula similar to 7, but an unusal structure was suggested to have two η^1 -dppm and one CO groups at one Ru atom and three CO groups at the other metal atom, probably on the basis of a typical AA'XX' spin system observed

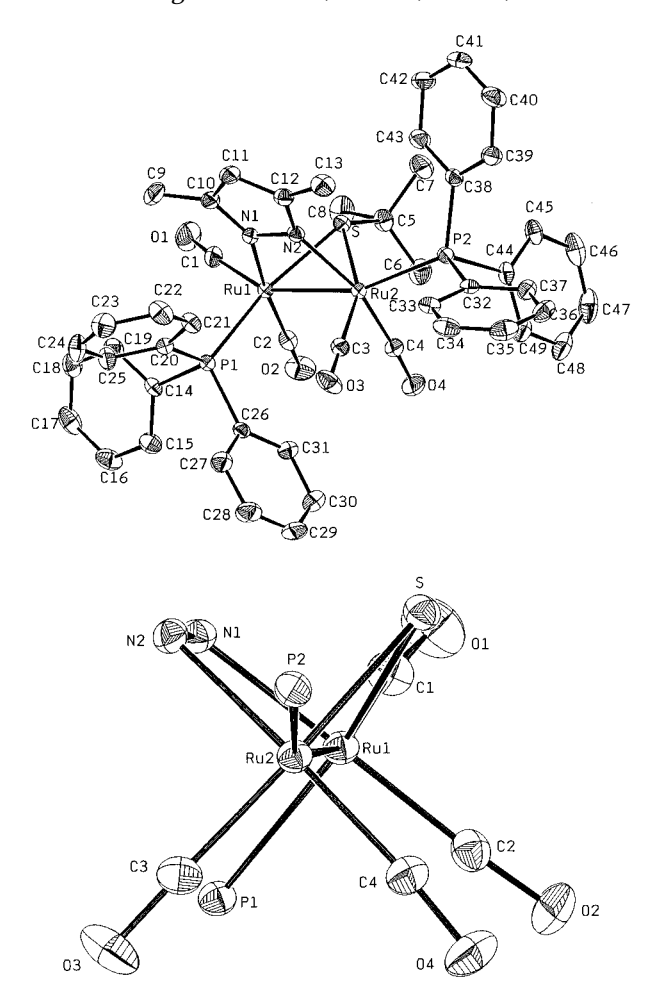


Figure 3. (a) Top: ORTEP plot of 10 with 50% thermal ellipsoids. (b) Bottom: ORTEP plot of 10 along the Ru-Ru axis with phenyl and tert-butyl groups omitted.

in a ³¹P{¹H} NMR spectrum.^{2d} However, such a suggestion was questioned, on the basis of our findings that the μ -Pz' linkage is rather strong and resistant even with respect to a strong nucleophile such as a thiolate anion and that the axial groups in $[Ru_2(\eta^2-L)_2(CO)_6]$, $[Ru_2(CO)_4(MeCN)_6]^{2+}$, or **1–3** are substitution labile. In order to obtain a clear-cut conclusion, we attempted a similar substitution reaction by following their reaction condition, i.e., by heating a mixture of 3 and excess dppm in THF for more than 24 h. The compound we obtained shows very similar IR and ¹H-NMR spectral data to those reported by Süss-Fink's group. It also exhibits two multiplets consistent with an AA'XX' spin system at δ 11.41 and -30.26, but these two values differ about 3.6-4.0 ppm from those reported. Further, the elemental analysis results clearly indicate that the compound should not be formulated as [Ru₂(Pz')₂(CO)₄- $(dppm)_2$ but $[Ru_2(Pz')_2(CO)_2(dppm)_2]$ (11) with only two, rather than four, carbonyls suggested. The crystal structure of 11 was hence determined to support this formulation. As shown in the simplified ORTEP plot of 11 (Figure 4), each Ru atom of 11 has one chelate dppm and one CO. The two carbonyls, C(1)O(1) and C(2)O(2), are in a gauche conformation with the torsion angle $\angle C(1)$ -Ru(1)-Ru(2)-C(2) = 85.9°. Obviously the bidentate ligand dppm can replace only the axial HPz' and carbonyl groups rather than cleave one or two apparently strong μ -Pz' linkages in **3** (Scheme 4).

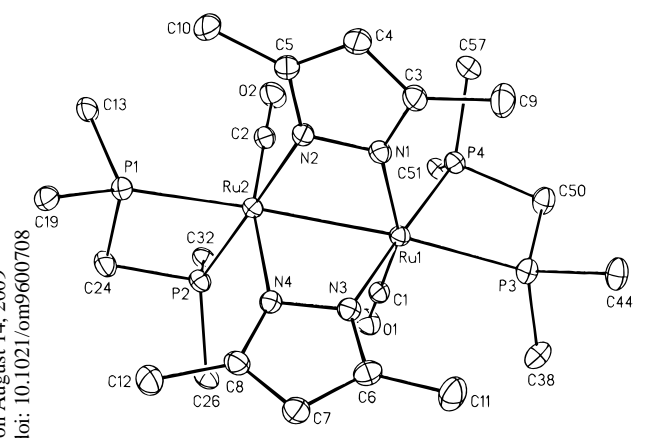
⁽⁵⁾ Sherlock, S. J.; Cowie, M.; Singleton, E.; Steyn, M. M. d. V. Organometallics 1988, 7, 1663.

Table 1. Selected Bond Lengths (Å) and Angles (deg)

| | Table 1. Selected | i Dona Lei | iguis (A) and An | gies (deg) | | |
|---|--|--|---|--|--|---|
| 2.682(1) 2.111(7) 1.82(1) 2.103(7) 1.839(10) | C(7)-O(4) C(20)-O(6) | 2.170(5) 1.135(10) 1.155(10) 1.252(10) | gths for 2 Ru(1)-N(2) Ru(1)-C(5) Ru(1)-O(5) Ru(2)-N(5) Ru(2)-C(7) | 2.261(7) 1.846(10) 2.170(6) 2.213(7) 1.850(10) | C(4)-O(1) C(6)-O(3) C(20)-O(5) N(1)-N(2) N(5)-N(6) | 1.17(1) 1.160(10) 1.278(10) 1.362(9) 1.341(9) |
| 162.2(2) 84.3(2) 123.6(8) 92.1(3) | O(6)-Ru(2)-C(7) C(6)-Ru(2)-N(4) Ru(1)-C(5)-O(2) Ru(2)-C(7)-O(4) | 178.1(3) 169.5(3) 179.0(8) 178.9(9) | Ru(1)-Ru(2)-N(5) Ru(1)-Ru(2)-O(6) O(5)-Ru(1)-C(5) C(4)-Ru(1)-N(3) | 160.0(2) 83.7(1) 178.6(3) 167.9(3) | C(7)-Ru(2)-C(6) Ru(1)-C(4)-O(1) Ru(2)-C(6)-O(3) | 88.1(4) 176.5(9) 178.3(9) |
| 2.7261(9) 2.129(6) 1.871(8) 2.4324(21) 1.828(8) | Ru(2)-O(6) C(5)-O(6) C(2)-O(2) C(4)-O(4) Ru(1)-P(1) | Bond Leng 2.136(5) 1.246(8) 1.134(9) 1.140(9) 2.4357(21) | gths for 5 Ru(1)-C(1) Ru(1)-O(5) Ru(2)-N(2) Ru(2)-C(4) | 1.834(9) 2.142(5) 2.127(6) 1.865(7) | C(5)-O(5) C(1)-O(1) C(3)-O(3) N(1)-N(2) | 1.265(9) 1.142(11) 1.147(10) 1.379(8) |
| 166.35(7) 83.66(13) 125.1(7) 89.8(4) | O(6)-Ru(2)-C(3) C(4)-Ru(2)-N(2) Ru(1)-C(2)-O(2) Ru(2)-C(4)-O(4) | Bond Ang 174.8(3) 164.8(3) 179.2(8) 177.7(8) | gles for 5 Ru(1)-Ru(2)-P(2) Ru(2)-Ru(1)-O(5) O(5)-Ru(1)-C(1) C(2)-Ru(1)-N(1) | 167.04(6) 82.94(13) 176.0(3) 166.4(3) | C(3)-Ru(2)-C(4) Ru(1)-C(1)-O(1) Ru(2)-C(3)-O(3) | 92.4(3) 178.8(7) 175.8(7) |
| 2.7469(5) 2.3795(10) 1.906(4) 2.4261(10) | Ru(2)-N(2) Ru(2)-C(4) C(1)-O(1) C(3)-O(3) | 2.153(3) 1.859(4) 1.136(6) 1.146(5) | $\begin{array}{l} Ru(1) - P(1) \\ Ru(1) - N(1) \\ Ru(1) - C(2) \\ Ru(2) - S \end{array}$ | 2.3735(10) 2.095(3) 1.865(4) 2.4276(10) | Ru(2)-C(3) N(1)-N(2) C(2)-O(2) C(4)-O(4) | 1.871(4) 1.375(4) 1.144(5) 1.139(5) |
| 103.54(3) 69.69(3) 154.94(12) 172.98(15) | Ru(1)-Ru(2)-C(4) N(2)-Ru(2)-C(4) Ru(1)-C(2)-O(2) Ru(2)-C(4)-O(4) | 92.43(12) 162.97(4) 176.0(4) 175.5(4) | Ru(1)-Ru(2)-P(2) C(1)-Ru(1)-C(2) Ru(2)-Ru(1)-C(2) Ru(1)-Ru(2)-C(3) | 88.32(18) 102.05(12) | Ru(1)-C(1)-O(1) Ru(2)-C(3)-O(3) | 171.2(4) |
| 2.738(1) 2.309(1) 2.112(3) 2.386(1) | $\begin{array}{l} Ru(2) - N(2) \\ Ru(2) - C(2) \\ C(2) - O(2) \\ N(3) - N(4) \end{array}$ | 2.120(3) 1.828(4) 1.168(5) 1.371(4) | $\begin{array}{c} Ru(1) - P(3) \\ Ru(1) - N(1) \\ Ru(1) - C(1) \\ Ru(2) - P(2) \end{array}$ | 2.416(1) 2.136(3) 1.846(4) 2.316(1) | Ru(2)-N(4) C(1)-O(1) N(1)-N(2) | 2.169(3) 1.150(5) 1.368(4) |
| 175.6(1) 176.1(1) 95.6(1) | P(1)-Ru(2)-P(2) C(2)-Ru(2)-N(4) Ru(1)-C(1)-O(1) | Bond Angl 72.0(1) 164.5(2) 176.7(3) | les for 11 P(3)-Ru(1)-P(4) C(1)-Ru(1)-N(1) Ru(1)-Ru(2)-P(1) | 72.3(1) 157.5(1) 172.3(1) | P(2)-Ru(2)-N(2) C(2)-Ru(2)-N(2) Ru(2)-C(2)-O(2) | 177.5(1) 88.7(1) 178.4(3) |
| 2.701(1) 2.009(6) 2.196(5) 2.097(5) 1.866(8) | Ru(2)-C(25) Ru(2)-N(3) C(26)-O(3) C(25)-O(2) Ru(1)-C(26) | Bond Leng 2.009(6) 2.192(4) 1.136(9) 1.178(9) 1.868(7) | ths for 12 Ru(1)-C(25) Ru(1)-N(2) N(5)-N(6) Ru(2)-C(24) | 2.016(9) 2.194(7) 1.365(8) 2.033(8) | Ru(2)-N(6) Ru(2)-N(4) C(27)-O(4) C(24)-O(1) | 2.093(5) 2.192(6) 1.133(10) 1.184(8) |
| 83.9(3) 93.4(3) 169.4(3) 168.9(2) | N(1)-Ru(1)-N(2) N(5)-Ru(1)-C(26) Ru(1)-C(26)-O(3) Ru(1)-C(25)-Ru(2) | 74.2(2) 174.5(3) 177.4(8) 84.3(3) | C(24)-Ru(2)-C(25) C(24)-Ru(2)-N(4) C(25)-Ru(2)-N(3) | 92.9(3) 170.4(2) 167.9(3) | N(3)-Ru(2)-N(4) N(6)-Ru(2)-C(27) Ru(2)-C(27)-O(4) | 74.0(2) 174.6(3) 177.6(8) |
| 2.6953(5) 2.024(4) 2.185(4) 2.124(4) 1.862(5) | $\begin{array}{c} Ru(2)-C(6) \\ Ru(2)-N(5) \\ C(1)-O(1) \\ C(5)-O(5) \\ Ru(1)-C(1) \end{array}$ | Bond Lengt 2.016(4) 2.209(4) 1.136(6) 1.177(5) 1.880(5) | hs for 14A Ru(1)-C(6) Ru(1)-N(2) N(3)-N(4) Ru(2)-C(5) | 2.008(5) 2.197(4) 1.383(5) 2.017(4) | Ru(2)-N(4) Ru(2)-N(6) C(2)-O(2) C(6)-O(6) | 2.132(4) 2.196(4) 1.149(6) 1.182(5) |
| 83.7(2) 94.6(2) 170.6(2) 167.6(2) | N(1)-Ru(1)-N(2) N(3)-Ru(1)-C(1) Ru(1)-C(1)-O(1) Ru(1)-C(6)-Ru(2) | Bond Angle 74.23(14) 172.5(2) 176.8(4) 84.1(2) | es for 14A C(5)-Ru(2)-C(6) C(5)-Ru(2)-N(5) C(6)-Ru(2)-N(6) | 169.3(2) | N(4)-Ru(2)-C(2) | 73.71(14) 171.5(2) 176.0(4) |
| 2.685(1) 2.191(4) 1.873(6) 2.013(6) 1.188(8) | $\begin{array}{c} Ru(2) - N(3) \\ Ru(2) - N(5) \\ Ru(2) - C(3) \\ C(2) - O(2) \\ Ru(1) - N(1) \end{array}$ | Bond Leng 2.198(4) 2.141(5) 1.997(6) 1.144(9) 2.200(4) | ths for 15 Ru(1)-N(6) Ru(1)-C(3) C(1)-O(1) C(4)-O(4) | 2.103(4) 2.026(6) 1.134(8) 1.175(8) | Ru(2)-N(4) Ru(2)-C(2) Ru(2)-C(4) N(5)-N(6) | 2.185(4) 1.851(7) 2.025(6) 1.393(6) |
| | 2.111(7) 1.82(1) 2.103(7) 1.839(10) 162.2(2) 84.3(2) 123.6(8) 92.1(3) 2.7261(9) 2.129(6) 1.871(8) 2.4324(21) 1.828(8) 166.35(7) 83.66(13) 125.1(7) 89.8(4) 2.7469(5) 2.3795(10) 1.906(4) 2.4261(10) 103.54(3) 69.69(3) 154.94(12) 172.98(15) 2.738(1) 2.309(1) 2.112(3) 2.386(1) 175.6(1) 176.1(1) 95.6(1) 175.6(1) 176.1(1) 95.6(1) 2.701(1) 2.009(6) 2.196(5) 2.097(5) 1.866(8) 83.9(3) 93.4(3) 169.4(3) 169.4(3) 168.9(2) 2.6953(5) 2.024(4) 2.124(4) 1.862(5) 83.7(2) 94.6(2) 170.6(2) 167.6(2) 2.685(1) 2.191(4) 1.873(6) 2.013(6) | 2.682(1) Ru(2)-O(6) 2.111(7) C(5)-O(2) 1.82(1) C(7)-O(4) 2.103(7) C(20)-O(6) 1.839(10) N(3)-N(4) 162.2(2) O(6)-Ru(2)-C(7) 84.3(2) C(6)-Ru(2)-N(4) 123.6(8) Ru(1)-C(5)-O(2) 92.1(3) Ru(2)-C(7)-O(4) 2.7261(9) Ru(2)-O(6) 2.129(6) C(5)-O(6) 1.871(8) C(2)-O(2) 2.4324(21) C(4)-O(4) 1.828(8) Ru(1)-P(1) 166.35(7) O(6)-Ru(2)-C(3) 83.66(13) C(4)-Ru(2)-N(2) 125.1(7) Ru(1)-C(2)-O(2) 89.8(4) Ru(2)-C(4)-O(4) 2.7469(5) Ru(2)-N(2) 89.8(4) Ru(2)-C(4) 1.906(4) C(1)-O(1) 2.4261(10) C(3)-O(3) 103.54(3) Ru(1)-Ru(2)-C(4) 1.906(4) C(1)-O(1) 2.738(1) Ru(2)-C(4)-O(4) 2.738(1) Ru(2)-C(4)-O(4) 2.738(1) Ru(2)-C(2) 2.112(3) C(2)-O(2) 2.309(1) Ru(2)-C(2) 2.112(3) C(2)-O(2) 2.386(1) N(3)-N(4) 175.6(1) P(1)-Ru(2)-P(2) 176.1(1) C(2)-Ru(2)-N(4) 95.6(1) Ru(1)-C(1)-O(1) 2.701(1) Ru(2)-C(25) 2.009(6) Ru(2)-N(3) 2.196(5) C(26)-O(3) 2.097(5) C(25)-O(2) 1.866(8) Ru(1)-C(26) 83.9(3) N(1)-Ru(1)-N(2) 93.4(3) N(5)-Ru(1)-C(26) 1.866(8) Ru(1)-C(26) 83.9(3) N(1)-Ru(1)-N(2) 93.4(3) N(5)-Ru(1)-C(26) 1.866(8) Ru(1)-C(26) 83.9(3) N(1)-Ru(1)-N(2) 94.6(2) N(3)-Ru(1)-C(1) 170.6(2) Ru(1)-C(1) 83.7(2) N(1)-Ru(1)-N(2) 94.6(2) N(3)-Ru(1)-C(1) 170.6(2) Ru(1)-C(1) 170.6(2) Ru(1)-C(1) 170.6(2) Ru(1)-C(1) 170.6(2) Ru(1)-C(1) 170.6(2) Ru(1)-C(1) 2.685(1) Ru(2)-N(5) 1.874(6) Ru(2)-N(6) 2.013(6) C(2)-O(2) | 2.682(1) Ru(2)-O(6) 2.170(5) 2.111(7) C(5)-O(2) 1.135(10) 1.82(1) C(7)-O(4) 1.155(10) 1.82(1) C(7)-O(4) 1.155(10) 1.839(10) N(3)-N(4) 1.376(8) Bond Ang 162.2(2) O(6)-Ru(2)-C(7) 178.1(3) 184.3(2) C(6)-Ru(2)-N(4) 169.5(3) 123.6(8) Ru(1)-C(5)-O(2) 179.0(8) 92.1(3) Ru(2)-C(7)-O(4) 178.9(9) 92.1(3) Ru(2)-O(6) 2.136(5) 2.129(6) C(5)-O(6) 1.246(8) 1.871(8) C(2)-O(2) 1.134(9) 2.4324(21) C(4)-O(4) 1.140(9) 1.828(8) Ru(1)-P(1) 2.4357(21) Bond Ang 166.35(7) O(6)-Ru(2)-C(3) 174.8(3) 125.1(7) Ru(1)-C(2)-O(2) 179.2(8) 83.66(13) C(4)-Ru(2)-N(2) 164.8(3) 125.1(7) Ru(1)-C(2)-O(2) 179.2(8) 89.8(4) Ru(2)-C(4)-O(4) 177.7(8) Bond Leng 2.7469(5) Ru(2)-C(4) 1.859(4) 1.906(4) C(1)-O(1) 1.136(6) 2.136(5) 2.3795(10) Ru(2)-C(4) 1.859(4) 1.906(4) C(1)-O(1) 1.136(6) 2.4261(10) C(3)-O(3) 1.146(5) Ru(2)-Ru(2)-C(4) 18.859(4) 1.906(4) C(1)-O(1) 1.136(6) 2.13(3) Ru(1)-Ru(2)-C(4) 162.97(4) 154.94(12) Ru(1)-C(2)-O(2) 176.0(4) 172.98(15) Ru(2)-C(4) 162.97(4) 154.94(12) Ru(1)-C(2)-O(2) 176.0(4) 172.98(15) Ru(2)-C(2) 1.828(4) 2.112(3) C(2)-O(2) 1.168(5) 2.386(1) N(3)-N(4) 1.371(4) Bond Ang 175.6(1) P(1)-Ru(2)-P(2) 176.0(4) 176.1(1) C(2)-Ru(2)-N(4) 164.5(2) 93.4(3) N(5)-Ru(1)-C(1) 176.7(3) 2.791(1) Ru(2)-C(2) 1.178(9) 1.75.6(1) Ru(1)-C(1)-O(1) 176.7(3) 2.009(6) Ru(2)-N(3) 2.192(4) 2.196(5) C(26)-O(3) 1.136(9) 2.097(5) C(25)-O(2) 1.178(9) 1.866(8) Ru(1)-C(26)-O(3) 177.4(8) 168.9(2) Ru(1)-C(1)-O(1) 176.5(2) 176.6(2) Ru(1)-C(1)-O(1) 176.8(4) 2.194(4) Ru(2)-N(5) 2.209(4) 2.195(5) C(25)-O(5) 1.177(5) 1.866(8) Ru(1)-C(1)-O(1) 172.5(2) 176.6(2) Ru(1)-C(1)-O(1) 176.8(4) 2.194(4) Ru(2)-N(5) 2.209(4) 2.195(6) C(2)-O(2) 1.174.5(3) 1.873(6) Ru(2)-C(3) 1.1997(6) 2.013(6) C(2)-O(2) 1.1144(9) | $ \begin{array}{c c c c c c c c c c c c c c c c c c c $ | $ \begin{array}{c c c c c c c c c c c c c c c c c c c $ | $ \begin{array}{c c c c c c c c c c c c c c c c c c c $ |

Table 1 (Continued)

| | | | Bond Ang | les for 15 | | | |
|-------------------|-----------|------------------|-----------|-----------------|-----------|------------------|-----------|
| Ru(1)-C(3)-Ru(2) | 83.7(2) | N(1)-Ru(1)-N(2) | 75.6(2) | C(3)-Ru(2)-C(4) | 95.2(2) | N(3)-Ru(2)-N(4) | 75.0(2) |
| C(3)-Ru(1)-C(4) | 94.7(2) | N(6)-Ru(1)-C(1) | 172.7(2) | C(3)-Ru(2)-N(4) | 169.4(2) | N(5)-Ru(2)-C(2) | 173.6(2) |
| C(3)-Ru(1)-N(2) | 168.8(2) | Ru(1)-C(1)-O(1) | 176.8(6) | C(4)-Ru(2)-N(3) | 168.1(2) | Ru(2)-C(2)-O(2) | 178.5(6) |
| C(4)-Ru(1)-N(1) | 171.1(2) | Ru(1)-C(4)-Ru(2) | 83.4(2) | | | | |
| | | | Bond Leng | othe for 16 | | | |
| D (4) T(4) | 0.704(0) | D (0) N(0) | | | 0.000(0) | D (0) NI(4) | 0.447(40) |
| Ru(1)-I(1) | 2.731(2) | Ru(2)-N(2) | 2.113(11) | I(2)-I(3) | 2.926(2) | Ru(2)-N(4) | 2.147(13) |
| Ru(2)-I(1) | 2.733(1) | Ru(2)-C(9) | 1.868(16) | I(3)-I(4) | 2.902(2) | Ru(2)-C(10) | 1.903(20) |
| Ru(1)-P(1) | 2.386(4) | C(7) - O(1) | 1.131(19) | Ru(1)-N(1) | 2.123(13) | C(8) - O(2) | 1.153(25) |
| Ru(1)-N(3) | 2.105(10) | C(9) - O(3) | 1.140(21) | Ru(1)-C(7) | 1.877(15) | C(10) - O(4) | 1.124(24) |
| Ru(1)-C(8) | 1.869(20) | N(1)-N(2) | 1.360(16) | Ru(2)-P(2) | 2.398(4) | N(3)-N(4) | 1.347(16) |
| | | | Dand Ann | dan fan 10 | | | |
| - (1) - (1) - (n) | 0= 4(4) | G(E) E (1) G(E) | Bond Ang | | | G(a) B (a) G(1a) | 00.0(0) |
| Ru(1)-I(1)-Ru(2) | 87.1(1) | C(7)-Ru(1)-C(8) | 90.8(7) | I(1)-Ru(1)-P(1) | 177.5(1) | C(9)-Ru(2)-C(10) | 89.6(8) |
| I(1)-Ru(2)-P(2) | 178.9(1) | Ru(1)-C(7)-O(1) | 175.8(14) | I(2)-I(3)-I(4) | 173.9(1) | Ru(1)-C(8)-O(2) | 173.9(14) |
| N(1)-Ru(1)-N(3) | 88.2(4) | Ru(2)-C(9)-O(3) | 174.1(11) | N(2)-Ru(2)-N(4) | 88.7(5) | Ru(2)-C(10)-O(4) | 174.0(17) |



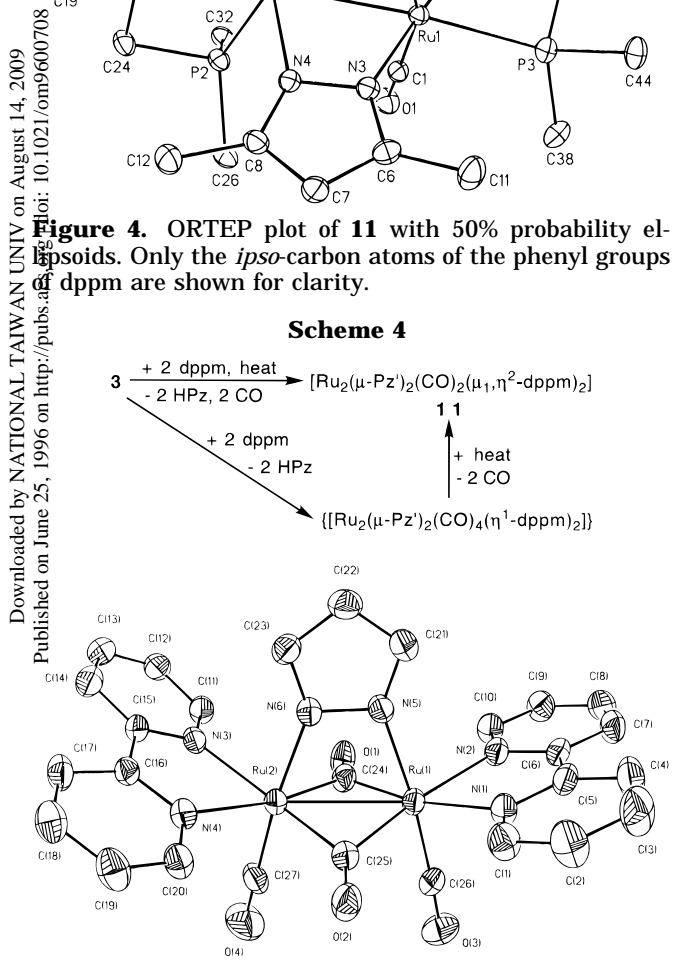


Figure 5. ORTEP plot of [12]+ with 30% thermal ellipsoids.

Consistent with the structure of **10** (Figure 3b), phosphine groups can occupy the equatorial sites if necessary.

However, excepting the replacement of the axial HL groups, the less-flexible bidentate ligands such as bpy and phen can cleave one μ -O₂CMe or μ -L bridge, but without losing any carbonyl in 1-3, to afford [Ru₂(μ -

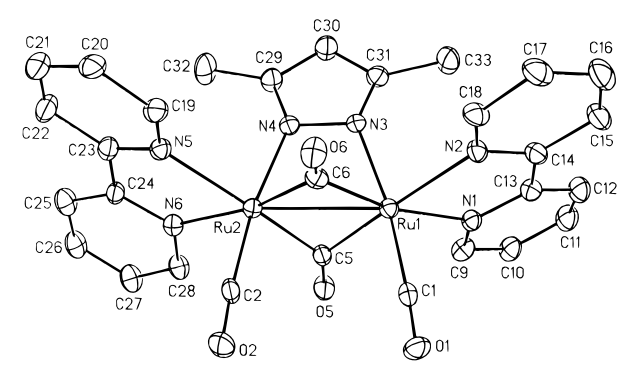


Figure 6. ORTEP plot of [14A]+ with 50% probability ellipsoids.

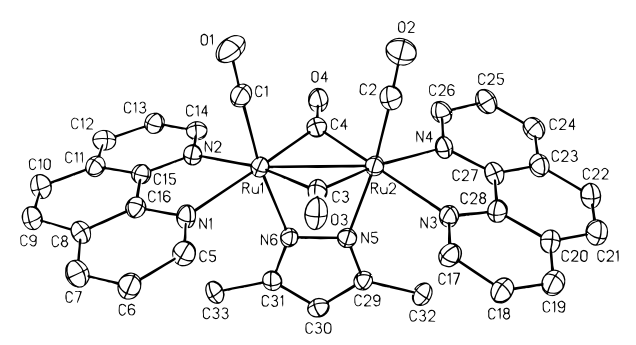


Figure 7. ORTEP plot of [15]⁺ with 50% probability ellipsoids.

Scheme 5

 $L(\mu-CO)_2(CO)_2(\mu_1,\eta^2-(N-N))_2$ (L = Pz, N-N = bpy $([12]^+)$, phen $([13]^+)$; L = Pz', N-N = bpy $([14]^+)$, phen $([15]^+)$) (Scheme 5). The crystal structures of 12, 14, and 15 were carried out to confirm the formulation, and it was found that in each asymmetric unit of the crystal used were two similar diruthenium molecules, 14A and 14B, found for 14, although only one dimer was observed for 12 and 15. The structures of $[12]^+$, $[14A]^+$, and $[15]^+$ are shown in Figures 5–7, respectively. Apparently the more severe steric effect required by bpy

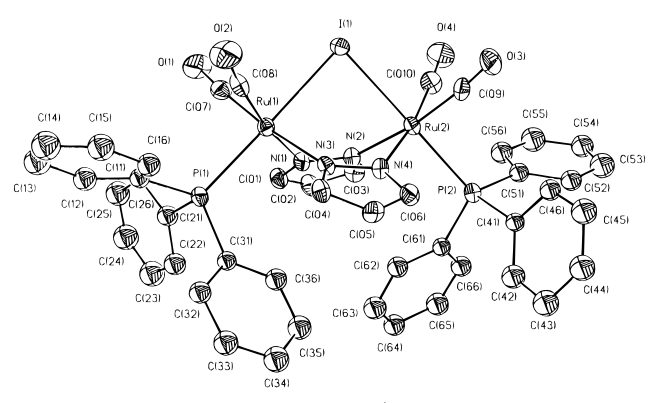


Figure 8. ORTEP plot of [16]⁺ with 50% probability ellipsoids.

and phen, relative to dppm, ^{5,6} results in a geometry in **12–15** totally different from that in **11**.

The μ -O₂CMe linkage was previously reported to be cleavable, and the product $[Ru_2(\mu-O_2CMe)(\mu-CO)_2(CO)_2 (\mu_1, \eta^2 - (N-N))_2$ + can be obtained from the reaction of catena-[Ru(O₂CMe)(CO)₂] with bpy or phen in EtOH.⁷ Here we wish to add that the apparently strong μ -L Enkage, previously reported to be a stable bridge in all **@**irhodium and -iridium complexes,¹ can be *cleaved*. The geaction between the heterobridged dimer 2 and N-N $\stackrel{\bullet}{\text{efid}}$ not give a mixture of $[\text{Ru}_2(\mu\text{-O}_2\text{CMe})(\mu\text{-CO})_2(\text{CO})_2\text{-}$ $[\alpha_1, \eta^2 - (N-N))_2]^+$ and $[Ru_2(\mu-L)(\mu-CO)_2(CO)_2(\mu_1, \eta^2 - (N-L))]_2$ $(\mathbf{N})_2$ but only the latter one, consistent with the ϵ weaker μ -acetato linkage compared with the μ -Pz'

weaker μ -acetato linkage compared with the μ -Pz \geq linkage, and the cleaving process is also selective when \geq linkage, and \geq linkage \geq linkage, and \geq linkage \geq linkage, and \geq linkage \geq linkage, an $\angle N(3) - C(15) - C(16) - N(4)$ in **12**, less than 6.4°. The identical distance of 2.701(1) Å found in both cations $\mathbf{f2}^+$ and $[\mathrm{Ru}_2(\mu\text{-}\mathrm{O}_2\mathrm{CMe})(\mu\text{-}\mathrm{CO})_2(\mathrm{CO})_2(\mu_1,\eta^2\text{-}\mathrm{bpy})_2]^+$ probably indicates a $\mu\text{-}\mathrm{O}_2\mathrm{CMe}$ linkage in a steric bulk similar a $\mu\text{-}\mathrm{Pz}$ linkage and further supports the facile Elentical distance of 2.701(1) A found in both cations Explacement of two μ -O₂CMe linkages in 1 by μ -Pz groups to give 4 (Scheme 1).

Reactions with Electrophiles. Electrophiles such as I₂ can react with **4**. However, it was strange to find that the reaction should consume up to 2 equiv of I₂ to complete the reaction for every dinuclear compound 4. Later, the crystal structure of the product compound was revealed to have an I₃⁻ as a counterion for [Ru₂(µ- $Pz)_2(\mu-I)(CO)_4(PPh_3)_2|^+$ ([16]⁺; cf., Figure 8 and Scheme 6). Though with two μ -Pz linkages, the two Ru atoms are separated by 3.762(2) Å, indicating no metal-metal bonding interactions. Obviously, the electrophilic reagent I2 can cleave the Ru-Ru bond and raise the oxidation state of each Ru atom, but cannot break the μ -azolato linkage. Such a feature was previously ob-

Scheme 6 [Ru₂(μ-Pz)₂(μ-I)(CO)₄(PPh₃)₂][I₃] $[Ru_2(CO)_4(MeCN)_6][BF_4]_2$ + 2 PPh₃

[Ru₂(CO)₄(MeCN)₄(PPh₃)₂][BF₄]₂

xs. Et₃O+BF₄

served in the dirhodium and -iridium systems¹ but not yet reported in the diruthenium system.² From the crystal structures of 2, 5, 10-12, and 14-16, it is apparent that the μ -azolato linkage is flexible to maintain two metal fragments in close proximity, both within and beyond the requirements of metal-metal interactions in the dimetal system.

From the aforementioned results, one or two μ -azolato linkages in 1-3 appear to be able to survive during a nucleophilic or electrophilic reaction (Schemes 1-5). However, some other reactions are present enabling removal of all the μ -acetato and -azolato linkages in the

An electrophilic reagent such as Et₃O⁺BF₄⁻ in the presence of MeCN was previously reported by our laboratory to convert a series of [Ru₂(CO)₄(μ-O₂CMe)₂- $(L')_2$] (L' = MeCN or phosphine (PR₃)) into [Ru₂(CO)₄- $(MeCN)_6][BF_4]_2$ and $[Ru_2(CO)_4(MeCN)_4(PR_3)_2][BF_4]_2$, probably involving an abstraction reaction by transformation of a μ -acetato bridge into the weakly coordinating ethyl acetate.4b We found that a similar reaction also occurs for 1-3 and 4-6 into [Ru₂(CO)₄(MeCN)₆]- $[BF_4]_2$ and $[Ru_2(CO)_4(MeCN)_4(PPh_3)_2][BF_4]_2$, respectively. The former product, $[Ru_2(CO)_4(MeCN)_6][B\bar{F}_4]_2$, can be converted by adding PPh3 into the latter one, $[Ru_2(CO)_4(MeCN)_4(PPh_3)_2][BF_4]_2$ (Scheme 6).^{4a}

Conclusion

Our investigation into the diruthenium carbonyl complexes containing the μ -azolato linkage resulted in the specific synthesis of 1-3 in satisfactory yield. Both nucleophilic and electrophilic reactions of 1-3 produce selectively one type of product containing either heteroor homobridges (Schemes 1-6) as confirmed in eight X-ray crystal structures (Figures 1–8). The μ -azolato linkage has been demonstrated to promote formation of novel compounds such as 11 and to maintain two ruthenium fragments in close proximity, both within and beyond the requirements of metal-metal interactions. More importantly, if necessary, the μ -azolato linkages can be cleaved partially by using the lessflexible bidentate nucleophiles such as bpy or phen or removed totally by using electrophiles such as trialkyloxonium reagents. The latter reaction can produce potentially versatile compounds such as [Ru₂(CO)₄- $(MeCN)_6][BF_4]_2$ and $[Ru_2(CO)_4(MeCN)_4(PPh_3)_2][BF_4]_2$.

Experimental Section

General Comments. All solvents were dried and purified by standard methods [ethers, paraffins, and arenes from potassium with benzophenone as indicator; halocarbons and acetonitrile from CaH₂; alcohols from the corresponding alkoxide] and were freshly distilled under nitrogen immediately before use. All reactions and manipulations were carried out in standard Schlenk ware, connected to a switchable double

^{(6) (}a) Puddephatt, R. J. Chem. Soc. Rev. **1983**, *12*, 99. (b) Balch, A. L. Homogeneous Catalysis with Metal Phosphine Complexes, Pignolet, L. H., Ed.; Plenum: New York, 1983; pp 167-213. (c) Chaudret, B.;

Delavaux, B.; Poilblanc, R. Coord. Chem. Rev. 1988, 86, 191. (7) (a) Steyn, M. M. d. V.; Singleton, E. Acta Crystallogr. 1988, C44, 1722. (b) Frediani, P.; Bianchi, M.; Salvini, A.; Guarducci, R.; Carluccio, L. C.; Piacenti, F.; Ianelli, S.; Nardelli, M. J. Organomet. Chem. 1993, *463*, 187.

manifold providing vacuum and nitrogen. Reagents and phosphines were used as supplied by either Aldrich or Strem. $^1\mathrm{H}$ and $^{31}\mathrm{P}$ NMR spectra were measured on a Bruker AM-200 ($^1\mathrm{H}$, 200 MHz), Bruker AMC-400, or Varian Unity Plus-400 ($^1\mathrm{H}$, 400 MHz; $^{31}\mathrm{P}$, 162 MHz) NMR spectrometer. $^1\mathrm{H}$ chemical shifts (δ in ppm, J in Hz) are defined as positive downfield relative to internal MeSi₄ (TMS) or the deuterated solvent, while $^{31}\mathrm{P}$ chemical shifts are defined as positive downfield relative to external 85% $\mathrm{H}_3\mathrm{PO}_4$. The IR spectra were recorded on a Hitachi Model 270–30 or Bio-Rad FTS 175 instrument. The following abbreviations were used: s, strong; m, medium; w, weak; s, singlet; d, doublet; t, triplet; dd, doublet of doublet; br, broad unresolved signal. Microanalyses were carried out by the staff of the Microanalytical Service of the Department of Chemistry, National Cheng Kung University.

Synthesis of $[Ru_2(CO)_4(\mu-Pz)_2(HPz)_2]$ (1). In a 100-mL Schlenk flask was added catena-[Ru(O2CMe)(CO)2] (1.0 g, 2.33 mmol), HPz (0.83 g, 12.2 mmol), 5 mL of Et₃N, and 30 mL of EtOH at room temperature. The mixture was then heated under reflux for 2 h and cooled to room temperature. The solvent and Et₃N were removed under vacuum and the resulting solid residue was redissolved in 5 mL of MeOH. Upon addition of 50 mL of H2O, a milky yellow precipitate formed immediately, which was collected on a medium frit. Recrystallization from CH2Cl2/MeOH afforded the pure product in \$1% yield. Alternatively, as described below for 3, 1 can also $\label{eq:condition} \begin{tabular}{lll} \hline \& & prepared from $[Ru_2(CO)_4(MeCN)_6][BF_4]_2$ and HPz/Et_3N. \\ \hline \& & prepared from $[Ru_2(CO)_4(MeCN)_6][BF_4]_2$ and HPz/Et_3N. \\ \hline \& & prepared from $[Ru_2(CO)_4(MeCN)_6][BF_4]_2$ and HPz/Et_3N. \\ \hline \& & prepared from $[Ru_2(CO)_4(MeCN)_6][BF_4]_2$ and HPz/Et_3N. \\ \hline \& & prepared from $[Ru_2(CO)_4(MeCN)_6][BF_4]_2$ and HPz/Et_3N. \\ \hline \& & prepared from $[Ru_2(CO)_4(MeCN)_6][BF_4]_2$ and HPz/Et_3N. \\ \hline \& & prepared from $[Ru_2(CO)_4(MeCN)_6][BF_4]_2$ and HPz/Et_3N. \\ \hline \& & prepared from $[Ru_2(CO)_4(MeCN)_6][BF_4]_2$ and HPz/Et_3N. \\ \hline \& & prepared from $[Ru_2(CO)_4(MeCN)_6][BF_4]_2$ and HPz/Et_3N. \\ \hline \& & prepared from $[Ru_2(CO)_4(MeCN)_6][BF_4]_2$ and $[Ru_2(CO)_4(MeCN)_6][Ru_2(CO)_4(MeCN)_6][BF_4]_2$ and $[Ru_2(CO)_4(MeCN)_6][Ru_2(CO)_4(MeCN)_6][Ru_2(CO)_4(MeCN)_6][Ru_2(CO)_4(MeCN)_6][Ru_2(CO)_4(MeCN)_6][Ru_2(CO)_4(MeCN)_6][Ru_2(CO)_4(MeCN)_6][Ru_2(CO)_4(MeCN)_6][Ru_2(CO)_4(MeCN)_6][Ru_2(CO)_4(MeCN)_6][Ru_2(CO)_4(MeCN)_6][Ru_2(CO)_4(MeCN)_6][Ru_2(CO)_4(MeCN)_6][Ru_2(CO)_4(MeCN)_6][Ru_2(CO)_4(MeCN)_6][Ru_2(CO)_4(MeCN)_6][Ru_2(CO)_4(MeCN)_6][Ru_2(CO)_6$ ₹ Eound: C, 32.54; H, 2.39; N, 18.85. ¹H NMR (25 °C, 400 MHz, $\overline{\mathbf{a}}$ cetone- d_6): NH at 12.87 (br, 2 H); H³ or H⁵ on HPz at 8.10 $\frac{1}{2}$ acetone- d_6): NH at 12.87 (br, 2 H); H³ or H⁵ on HPz at 8.10 $\frac{1}{2}$ $\frac{1}{2}$ $\vec{\blacktriangleleft}$ on μ -Pz at 6.64 (m, 2 H,); H⁴ on μ -Pz at 6.02 (m, 2 H). IR: $\stackrel{\,}{ \mbox{\it E}}$ $\stackrel{\,}{ \mbox{\it E}}$ 2024 s, 1976 m, 1942 s cm⁻¹ in CH₂Cl₂; $v_{\rm NH}$, 3436 w; $v_{\rm CO}$, $\geq 2016 \text{ s}, 1964 \text{ m}, 1934 \text{ s cm}^{-1} \text{ in KBr}.$

Synthesis of $[\mathbf{Ru_2(CO)_4(\mu-Pz')(\mu-O_2CMe)(HPz')_2}]$ (2). The yellow compound 2 was prepared from catena- $[\mathbf{Ru(O_2-Me)(HPz')_2}]$ (2). Employed by Employed Brown (CO)₂] using HPz' in a procedure similar to that used for $(\mathbf{C_{11}H_{16}N_{6}O_{6}Ru_2)}$; C, 38.18; $(\mathbf{H}, 3.97; N, 12.72)$. Found: C, 38.51; H, 3.99; N, 12.39. H NMR $(\mathbf{Z_{25} ^{\circ}C}, 200 \text{ MHz}, \mathbf{CDCl_3})$; NH at 10.92 (br, 2 H); H⁴ on HPz' at 6.02 (s, 1 H), 6.01 (s, 1 H); H⁴ on $(\mathbf{\mu-Pz'})$ at 5.57 (s, 1 H); Me³ or Me⁵ on HPz' at 2.48 (br, 6 H), 2.29 (br, 6 H); Me³ or Me⁵ on $(\mathbf{\mu-Pz'})$ at 1.38 (br, 6 H); $(\mathbf{\mu-O_2CMe})$ at 2.15 (s, 3 H). IR: $(\mathbf{\nu_{CO}})$ at 1.392 4 s, 1974 m, 1940 s cm⁻¹ in CH₂Cl₂; $(\mathbf{\nu_{NH}})$ 3328 w, $(\mathbf{\nu_{CO}})$ 2024 $(\mathbf{\mu-Pz'})$ 1970 m, 1942 s cm⁻¹ in KBr.

5 Synthesis of $[Ru_2(CO)_4(\mu-Pz')_2(HPz')_2]$ (3). To the solu- $r_{\rm e}^2$ action of $[Ru_2(CO)_4(\mu-O_2CMe)_2(MeCN)_2]$ (0.28 mmol) with excess Et₃O+BF₄-,⁴ in a 100-mL Schlenk flask was added HPz' (0.14 g, 1.4 mmol), 1 mL of Et₃N, and 20 mL of MeOH at room temperature. The mixture was then heated under reflux for 2 h and cooled to room temperature. The volume of the solution was reduced to ca. 5 mL under vacuum. Upon addition of 40 mL of H₂O, a milky yellow precipitate formed immediately, which was collected on a medium frit. Recrystallization from CH2Cl2/MeOH afforded the pure product in 83% yield. Anal. Calcd for C₂₄H₃₀N₈O₄Ru₂: C, 41.38; H, 4.34; N, 16.08. Found: C, 41.35; H, 4.28; N, 15.83. 1H NMR (25 °C, 200 MHz, CDCl₃): NH at 9.80 (br, 2 H); H⁴ on HPz' at 6.05 (s, 1 H), 5.81 (s, 1 H); H⁴ on μ -Pz' at 5.31 (s, 1 H); Me³ or Me⁵ on HPz' at 2.55 (br, 6 H), 2.24 (br, 6 H); Me³ or Me⁵ on μ -Pz' at 1.55 (br, 12 H). IR: v_{CO} , 2016 s, 1968 m, 1934 s cm⁻¹ in CH_2Cl_2 ; v_{NH} , 3424 w, v_{CO} , 2012 s, 1960 m, 1928 s cm $^{-1}$ in

Reaction between 1 and PPh3. In a 100-mL Schlenk flask was added **1** (0.100 g, 0.17 mmol), PPh3 (0.18 g, 0.69 mmol), and 25 mL of MeCN at room temperature. The solution gradually formed pale yellow precipitate. After 0.5 h, the yellow solid was collected on a medium frit, washed three times with 5 mL of MeCN, and dried in vacuo to give 0.096 g (80%). This solid was identified as $[Ru_2(CO)_4(\mu-Pz)_2-V_2]$

 $(PPh_3)_2]$ by comparison of both the NMR and IR spectral evidences with those reported. 2c

Reaction between 2 and PPh₃. The yellow compound **5** was prepared from **2** in a procedure similar to that used for **4**. The yield is 97%. Anal. Calcd for C₄₇H₄₀N₂O₆P₂Ru₂: C, 56.85; H, 4.06; N, 2.82. Found: C, 56.78; H, 4.04; N, 2.72. ¹H NMR (25 °C, 200 MHz, CDCl₃): PPh₃ at 7.60 (br, 12 H), 7.40 (m, 18 H); H⁴ on μ-Pz' at 5.67 (s, 1 H); Me³ or Me⁵ on μ-Pz' at 1.57 (br, 6 H); μ-O₂C**Me** at 1.75 (s, 3 H). ³¹P{¹H} NMR (25 °C, 162 MHz, CDCl₃): 12.50 (s, 2 P). IR (CH₂Cl₂): $v_{\rm CO}$, 2028 s, 1982 m, 1954 s cm⁻¹.

Reaction between 3 and PPh₃. The yellow compound **6** was prepared from **3** in a procedure similar to that used for **4**. The yield is 94%. Anal. Calcd for $C_{50}H_{44}N_4O_4P_2Ru_2$: C, 58.36; H, 4.31; N, 5.44. Found: C, 58.29; H, 4.28; N, 5.57. ¹H NMR (25 , 200 MHz, CDCl₃): PPh₃ at 7.54–7.23 (m, 30 H); H⁴ on μ-Pz' at 5.63 (s, 1 H), 5.58 (s, 1 H); Me³ or Me⁵ on μ-Pz' at 2.27 (s, 3 H), 1.80 (s, 3 H), 1.51 (s, 3 H), 1.46 (s, 3 H). ³¹P{¹H} NMR (25 °C, 162 MHz, CDCl₃): 12.69 (s, 2 P). IR (CH₂Cl₂): $v_{\rm CO}$, 2016 s, 1990 m, 1944 s, 1924 m cm⁻¹.

Reaction between 1 and dppm. The yellow compound 7 was prepared from 1 using dppm in a procedure similar to that used for 4. The yield is 93%. Anal. Calcd for $C_{60}H_{50}$ N₄O₄P₄Ru₂: C, 59.22; H, 4.14; N, 4.60. Found: C, 59.28; H, 4.08; N, 4.59. ¹H NMR (25 °C, 200 MHz, CDCl₃): PPh₃ at 7.65–7.10 (m, 40 H); H³ and H⁵ on μ-Pz at 6.46 (d, 4 H, J = 2.2); H⁴ on μ-Pz at 5.63 (t, 2 H); CH₂ of dppm at 3.47 (m, 4 H). ³¹P{¹H} NMR (25 °C, 162 MHz, CDCl₃): 12.12 (m, 2 P), −26.18 (m, 2 P). IR (CH₂Cl₂): ν _{CO}, 2024 s, 1982 m, 1954 s cm⁻¹.

Reaction between 5 and NaPz, NaSPh, and NaStBu. A typical reaction is shown as follows. In a 100-mL Schlenk flask was added 5 (108 mg, 0.109 mmol), NaPz (0.30 g, 3.33 mmol), and 20 mL of THF at room temperature. The mixture was then heated under reflux for 4 h and cooled to room temperature. The solvent was removed under vacuum. Recrystallization from CH₂Cl₂/hexane afforded the pure product (8) in 85% yield. Anal. Calcd for $C_{48}H_{40}N_4O_4P_2Ru_2$: C, 57.59; H, 4.02; N, 5.59. Found: C, 57.65; H, 3.91; N, 5.54. ¹H NMR (25 °C, 200 MHz, CDCl₃): PPh₃ at 7.57 (br, 12 H), 7.39 (br, 18 H); H³ and H⁵ on μ -Pz at 6.89 (d, 2 H, J = 2.0); H⁴ on μ -Pz at 5.78 (t, 1 H); H⁴ on μ -Pz' at 5.61 (s, 1 H); Me³ and Me⁵ on μ -Pz' at 1.56 (s, 6 H). ³¹P{¹H} NMR (25 °C, 162 MHz, CDCl₃): 12.12 (s, 2 P). IR (CH₂Cl₂): v_{CO} , 2028 s, 1986 m, 1958 s cm⁻¹. Compound 9 was prepared from 5 using NaSPh in a procedure similar to that used for 8. The yield is 87%. Anal. Calcd for C₅₁H₄₂N₂O₄P₂Ru₂S: C, 58.72; H, 4.05; N, 2.69. Found: C, 58.76; H, 3.94; N, 2.78. ¹H NMR (25 °C, 200 MHz, CDCl₃): PPh₃ at 7.38 (br, 12 H), 7.27 (m, 18 H); SPh at 6.81 (m, 5 H); H^4 on μ -Pz' at 5.42 (s, 1 H); Me^3 and Me^5 on μ -Pz' at 1.26 (s, 6 H). ³¹P{¹H} NMR (25 °C, 162 MHz, CDCl₃): 24.66 (s, 2 P). IR (CH₂Cl₂) v_{CO} , 2016 s, 1982 m, 1946 s cm⁻¹. Compound **10** was prepared from 5 using NaStBu in a procedure similar to that used for 8. The yield is 90%. Anal. Calcd for C₄₉H₄₄-N₂O₄P₂Ru₂S: C, 57.53; H, 4.53; N, 2.74. Found: C, 57.33; H, 4.34; N, 2.69. ¹H NMR (25 °C, 200 MHz, CDCl₃): PPh₃ at 7.55–7.26 (m, 30 H); H⁴ on μ -Pz' at 5.23 (s, 1 H); Me³ and Me⁵ on μ -Pz' at 1.54 (br, 6 H); S^tBu at 1.12 (s, 9 H). ${}^{31}P\{{}^{1}H\}$ NMR $(25 \, ^{\circ}\text{C}, 162 \, \text{MHz}, \text{CDCl}_3)$: $22.46 \, (d, 1 \, P, \, J = 8.7), 41.9 \, (d, 1 \, P)$. IR (CH₂Cl₂): v_{CO} , 2004 s, 1980 vs, 1934 s cm⁻¹.

Reaction between 3 and dppm. In a 100-mL Schlenk flask was added **3** (133 mg, 0.191 mmol), dppm (168 mg, 0.438 mmol), and 30 mL of THF at room temperature. The mixture was first stirred at this temperature for 10 min and then heated under reflux for 28 h, giving a clear orange-red solution. The solvent was removed under vacuum and the resulting solid redissolved in 40 mL of CH₂Cl₂. After filtration through a medium frit, the volume of the filtrate was reduced to ca. 15 mL. A 45 mL volume of hexane was carefully added on the top of the solution and the two-layer mixture was cooled to $-40~^{\circ}\text{C}$ for 1 week, giving orange-red crystals. The crystals were collected on a medium frit and dried in vacuo to give 157 mg of $[\text{Ru}_2(\mu\text{-Pz'})_2(\text{CO})_2(\mu_1,\eta^2\text{-dppm})_2]$ (11), containing a solvate

Table 2. Crystal Data

| | Tal | ole 2. Crystal Data | | | |
|---|--|---|---|---|--|
| | compd | | | | |
| | 2 | 5 | 10 | 11 | |
| formula | $C_{21}H_{26}N_6O_6Ru_2$ | $C_{47}H_{40}N_2O_6P_2Ru_2$ | C ₄₉ H ₄₆ N ₂ O ₄ P ₄ Ru ₂ S | $C_{63}H_{60}Cl_2N_4O_2P_4Ru_2$ | |
| fw | 660.61 | 992.92 | 1023.05 | 1302.1 | |
| color, habit | yellow, prism | orange, prism | orange, prism | orange, equant | |
| diffractometer used | Rigaku AFC6S | Nonius CAD4 | Nonium CAD4 | Siemens SMART-CCI | |
| space group | monoclinic, $P2_1/c$ | monoclinic, $P2_1/c$ | monoclinic, $P2_1/n$ | monoclinic, $P2_1/n$ | |
| a, Å | 14.069(5) | 10.4555(16) | 13.0086(18) | 13.970(3) | |
| b, Å | 13.288(3) | 16.113(3) | 17.363(3) | 25.737(5) | |
| c, Å | 14.545(3) | 26.063(4) | 20.945(3) | 16.826(3) | |
| β, deg | 98.25(2) | 91.420(13) | 104.251(12) | 92.65(3) | |
| V , $\mathring{\mathbf{A}}^3$ | 2691(1) | 4389.6(13) | 4585.3(12) | 6043(2) | |
| Z | 4 | 4 | 4 | 4 | |
| D_{calcd} , g cm ⁻³ | 1.630 | 1.502 | 1.482 | 1.431 | |
| $\lambda(Mo K\alpha), A$ | 0.710 69 | 0.710 69 | 0.710 69 | 0.710 73 | |
| F(000) | 1320 | 1998 | 2070 | 2656 | |
| unit cell detn: no. 2θ range, deg | | 25, 17-23 | 25, 17-26 | whole data | |
| scan type | ω -2 θ | θ -2 θ | θ -2 θ | hemisphere | |
| 2θ range, deg | 6-50 | 2-50 | 2-50 | 1-52 | |
| h,k,l range | $16,15,\pm 17$ | $\pm 12,19,30$ | $\pm 15,20,24$ | $\pm 17,31,20$ | |
| μ (Mo K α), cm ⁻¹ | 11.67 | 7.89 | 7.57 | 7.40 | |
| cryst size, mm | $0.41 \times 0.41 \times 0.66$ | $0.20\times0.20\times0.30$ | $0.30 \times 0.35 \times 0.35$ | $0.4 \times 0.4 \times 0.4$ | |
| temp, K | 296 | 298 | 298 | 297 | |
| no. of measd reflns | 5228 | 4227 | 8063 | 27 384 | |
| no. of unique reflns | 5014 | 4227 | 8063 | 10 543 | |
| $_{\infty}$ no. of obsd reflns (N ₀) | 3407 (>3 <i>σ</i>) | 2345 (>2σ) | 5956 (>2σ) | 7883 (≥3 <i>o</i>) | |
| $\stackrel{\sim}{\mathbb{R}}\!$ | 0.047, 0.048 | 0.044, 0.041 | 0.031, 0.031 | 0.038, 0.038 | |
| GOF ^a Grefinement program | 4.00 | 1.08 | 1.28 | 1.70 | |
| පූrefinement program | TEXSAN | NRCVAX | NRCVAX | SHELXTL-PLUS | |
| Eno. of ref params (N_p) | 316 | 532 | 542 | 695 | |
| weighting scheme | $[\sigma^2(F_0)]^{-1}$ | $[\sigma^2(F_0) + 0.0002F_0^2]^{-1}$ | $[\sigma^2(F_0) + 0.0001F_0^2]^{-1}$ | $[\sigma^2(F_0) + 0.0001F_0^2]^{-1}$ | |
| $\supseteq g \text{ (2nd ext coeff)} \times 10e^4$ | 0 | 0 | 0.95(4) | 0.000052(8) | |
| −5 (≈iid cxt cocii) × 10t | - | • | | , , | |
| $(\Delta \rho)_{\text{max}}$, e A^{-3} | 0.79 | 0.40 | 0.44 | 0.42 | |
| $(\Delta \rho)_{\text{max}}$, e A^{-3} | - | • | | , , | |
| $\mathfrak{S}(\Delta ho)_{\mathrm{max}}$, e $\mathring{\mathrm{A}}^{-3}$ $\mathfrak{S}(\Delta ho)_{\mathrm{min}}$, e $\mathring{\mathrm{A}}^{-3}$ | 0.79 | 0.40 -0.41 | 0.44 | 0.42 | |
| $\Xi(\Delta ho)_{ m max}$, e ${ m \mathring{A}}^{-3}$ $(\Delta ho)_{ m min}$, e ${ m \mathring{A}}^{-3}$ $\Xi(\Delta ho)_{ m min}$ $\Xi(\Delta ho)_{ m m$ | 0.79 | 0.40 -0.41 | 0.44 -0.36 | 0.42 | |
| $egin{array}{ccccc} egin{array}{ccccccccc} egin{array}{cccccccccccccccccccccccccccccccccccc$ | 0.79 -1.28 12 C ₅₂ H ₄₁ BCl ₂ N ₆ O ₄ Ru ₂ | 0.40 -0.41 con 14 C ₅₉ H ₄₈ Cl ₂ F ₁₂ N ₁₂ O ₈ P ₂ Ru ₄ | $\begin{array}{c} 0.44 \\ -0.36 \\ \\ \\ \\ \hline \textbf{npd} \\ \\ \hline \textbf{15} \\ \\ C_{34}H_{25}Cl_{2}F_{6}N_{2}O_{4}PRu_{2} \\ \end{array}$ | 0.42 -0.44 16 C _{47.5} H ₃₆ Cl ₃ I ₄ N ₄ O ₄ P ₂ Rt | |
| $\Xi(\Delta ho)_{ m max}$, e ${ m \mathring{A}}^{-3}$.: $(\Delta ho)_{ m min}$, e ${ m \mathring{A}}^{-3}$ $\Xi(\Delta ho)_{ m min}$, e ${ m \mathring{A}}^{-3}$ $\Xi(\Delta ho)_{ m min}$. | 0.79 -1.28 12 C ₅₂ H ₄₁ BCl ₂ N ₆ O ₄ Ru ₂ 1097.8 | $\begin{matrix} 0.40 \\ -0.41 \end{matrix}$ con $\begin{matrix} \textbf{14} \\ C_{59}H_{48}Cl_2F_{12}N_{12}O_8P_2Ru_4 \\ 1818.21 \end{matrix}$ | $\begin{array}{c} 0.44 \\ -0.36 \\ \\ \hline \\ \textbf{npd} \\ \hline \\ \textbf{25} \\ C_{34} \\ H_{25} \\ Cl_{2} \\ F_{6} \\ N_{2} \\ O_{4} \\ PRu_{2} \\ 999.6 \\ \end{array}$ | 0.42 -0.44 16 C _{47.5} H ₃₆ Cl ₃ I ₄ N ₄ O ₄ P ₂ Rt 1604.8 | |
| $\begin{picture}(200,0) \put(0,0){\line(0,0){$\stackrel{\frown}{\Omega}$}} \put(0,0$ | 0.79 -1.28 12 C ₅₂ H ₄₁ BCl ₂ N ₆ O ₄ Ru ₂ 1097.8 orange, rhombohedron | 0.40 -0.41 con 14 C ₅₉ H ₄₈ Cl ₂ F ₁₂ N ₁₂ O ₈ P ₂ Ru ₄ 1818.21 orange, equant | $\begin{array}{c} 0.44 \\ -0.36 \\ \\ \hline \\ \textbf{npd} \\ \hline \\ \textbf{LS} \\ C_{34}H_{25}Cl_{2}F_{6}N_{2}O_{4}PRu_{2} \\ 999.6 \\ \\ \text{yellow-brown, lamellar} \\ \end{array}$ | 0.42 -0.44 16 C _{47.5} H ₃₆ Cl ₃ I ₄ N ₄ O ₄ P ₂ Ru 1604.8 orange-brown, irregula | |
| $\begin{picture}(2000)(0,0) \put(0,0){\line(0,0){100}} \put(0,0){\line(0,0$ | 0.79 -1.28 12 C ₅₂ H ₄₁ BCl ₂ N ₆ O ₄ Ru ₂ 1097.8 orange, rhombohedron Siemens SMART-CCD | 0.40 -0.41 con 14 C ₅₉ H ₄₈ Cl ₂ F ₁₂ N ₁₂ O ₈ P ₂ Ru ₄ 1818.21 orange, equant Siemens SMART-CCD | $0.44\\ -0.36$ npd 15 $C_{34}H_{25}Cl_2F_6N_2O_4PRu_2\\ 999.6\\ yellow-brown, lamellar\\ Siemens SMART-CCD$ | 0.42 -0.44 16 C _{47.5} H ₃₆ Cl ₃ I ₄ N ₄ O ₄ P ₂ Rt 1604.8 orange-brown, irregula Siemens P4 | |
| $\begin{picture}(2000)(0,0) \put(0,0){\line(0,0){100}} \put(0,0){\line(0,0$ | 0.79 -1.28 12 C ₅₂ H ₄₁ BCl ₂ N ₆ O ₄ Ru ₂ 1097.8 orange, rhombohedron Siemens SMART-CCD triclinic, $P\bar{1}$ | 0.40 -0.41 14 C ₅₉ H ₄₈ Cl ₂ F ₁₂ N ₁₂ O ₈ P ₂ Ru ₄ 1818.21 orange, equant Siemens SMART-CCD triclinic, <i>P</i> I | 0.44 -0.36 npd 15 C ₃₄ H ₂₅ Cl ₂ F ₆ N ₂ O ₄ PRu ₂ 999.6 yellow-brown, lamellar Siemens SMART-CCD orthorhombic, <i>Pbca</i> | 0.42 -0.44 16 C _{47.5} H ₃₆ Cl ₃ I ₄ N ₄ O ₄ P ₂ Ru 1604.8 orange-brown, irregula Siemens P4 triclinic, PI | |
| $\begin{picture}(2000)(0,0) \put(0,0){\line(0,0){100}} \put(0,0){\line(0,0$ | 0.79 -1.28 12 C ₅₂ H ₄₁ BCl ₂ N ₆ O ₄ Ru ₂ 1097.8 orange, rhombohedron Siemens SMART-CCD triclinic, <i>P</i> I 10.712(4) | $\begin{array}{c} 0.40 \\ -0.41 \\ \hline \\ \textbf{14} \\ \hline \\ C_{59}H_{48}Cl_2F_{12}N_{12}O_8P_2Ru_4 \\ 1818.21 \\ \text{orange, equant} \\ \text{Siemens SMART-CCD} \\ \text{triclinic, } P\overline{1} \\ 14.4764(2) \\ \end{array}$ | 0.44 -0.36 npd 15 C ₃₄ H ₂₅ Cl ₂ F ₆ N ₂ O ₄ PRu ₂ 999.6 yellow-brown, lamellar Siemens SMART-CCD orthorhombic, <i>Pbca</i> 17.614(2) | 0.42 -0.44 16 C _{47.5} H ₃₆ Cl ₃ I ₄ N ₄ O ₄ P ₂ Ru 1604.8 orange-brown, irregula Siemens P4 triclinic, PI 11.744(1) | |
| $\begin{picture}(200,0) \put(0,0){\line(0,0){\mathbb{A}}} \put(0,$ | $\begin{array}{c} 0.79 \\ -1.28 \\ \hline \\ \hline & \textbf{12} \\ \hline \\ C_{52}H_{41}BCl_2N_6O_4Ru_2 \\ 1097.8 \\ orange, rhombohedron \\ Siemens SMART-CCD \\ triclinic, P\bar{\textbf{1}} \\ 10.712(4) \\ 13.939(4) \\ \end{array}$ | 0.40 -0.41 Con 14 C ₅₉ H ₄₈ Cl ₂ F ₁₂ N ₁₂ O ₈ P ₂ Ru ₄ 1818.21 orange, equant Siemens SMART-CCD triclinic, <i>P</i> I 14.4764(2) 15.0429(2) | $\begin{array}{c} 0.44\\ -0.36 \\ \\ \hline \text{npd} \\ \hline \\ \textbf{15} \\ \hline C_{34}H_{25}Cl_2F_6N_2O_4PRu_2\\ 999.6\\ \text{yellow-brown, lamellar} \\ \text{Siemens SMART-CCD} \\ \text{orthorhombic, } \textit{Pbca} \\ 17.614(2)\\ 13.624(2) \\ \end{array}$ | 0.42 -0.44 16 C _{47.5} H ₃₆ Cl ₃ I ₄ N ₄ O ₄ P ₂ Ru 1604.8 orange-brown, irregula Siemens P4 triclinic, PI 11.744(1) 13.357(1) | |
| $\begin{picture}(200,0) \put(0,0){\line(0,0){\mathbb{A}}} \put(0,$ | $\begin{array}{c} 0.79 \\ -1.28 \\ \hline \\ \hline & \textbf{12} \\ \hline \\ C_{52}H_{41}BCl_2N_6O_4Ru_2 \\ 1097.8 \\ \text{orange, rhombohedron} \\ \text{Siemens SMART-CCD} \\ \text{triclinic, } P\overline{1} \\ 10.712(4) \\ 13.939(4) \\ 17.871(7) \\ \end{array}$ | $\begin{array}{c} 0.40 \\ -0.41 \\ \hline \\ \hline & \textbf{14} \\ \hline \\ C_{59}H_{48}Cl_2F_{12}N_{12}O_8P_2Ru_4 \\ 1818.21 \\ \text{orange, equant} \\ \text{Siemens SMART-CCD} \\ \text{triclinic, } P\overline{1} \\ 14.4764(2) \\ 15.0429(2) \\ 17.0034(1) \\ \\ \end{array}$ | $\begin{array}{c} 0.44 \\ -0.36 \\ \\ \hline \text{npd} \\ \hline \\ \textbf{15} \\ \hline C_{34} H_{25} Cl_2 F_6 N_2 O_4 PRu_2 \\ 999.6 \\ \text{yellow-brown, lamellar} \\ \text{Siemens SMART-CCD} \\ \text{orthorhombic, } \textit{Pbca} \\ 17.614(2) \\ 13.624(2) \\ 31.294(2) \\ \end{array}$ | 0.42 -0.44 16 C _{47.5} H ₃₆ Cl ₃ I ₄ N ₄ O ₄ P ₂ Ru 1604.8 orange-brown, irregula Siemens P4 triclinic, PĪ 11.744(1) 13.357(1) 20.173(2) | |
| $\begin{picture}(200,0) \put(0,0){\line(0,0){\mathbb{A}}} \put(0,$ | $\begin{array}{c} 0.79 \\ -1.28 \\ \hline \\ \hline & \textbf{12} \\ \hline \\ C_{52}H_{41}BCl_2N_6O_4Ru_2 \\ 1097.8 \\ \text{orange, rhombohedron} \\ \text{Siemens SMART-CCD} \\ \text{triclinic, } P\overline{1} \\ 10.712(4) \\ 13.939(4) \\ 17.871(7) \\ 67.156(14) \\ \end{array}$ | $\begin{array}{c} 0.40 \\ -0.41 \\ \hline \\ \textbf{14} \\ \hline \\ \textbf{C}_{59}\textbf{H}_{48}\textbf{Cl}_{2}\textbf{F}_{12}\textbf{N}_{12}\textbf{O}_{8}\textbf{P}_{2}\textbf{Ru}_{4} \\ \textbf{1818.21} \\ \textbf{orange, equant} \\ \textbf{Siemens SMART-CCD} \\ \textbf{triclinic, } P\overline{\textbf{I}} \\ \textbf{14.4764(2)} \\ \textbf{15.0429(2)} \\ \textbf{17.0034(1)} \\ \textbf{97.829(1)} \\ \end{array}$ | $\begin{array}{c} 0.44 \\ -0.36 \\ \\ \hline \\ \text{npd} \\ \hline \\ \hline \\ C_{34}H_{25}Cl_{2}F_{6}N_{2}O_{4}PRu_{2} \\ 999.6 \\ \text{yellow-brown, lamellar} \\ \text{Siemens SMART-CCD} \\ \text{orthorhombic, } \textit{Pbca} \\ 17.614(2) \\ 13.624(2) \\ 31.294(2) \\ 90 \\ \end{array}$ | 0.42 -0.44 16 C _{47.5} H ₃₆ Cl ₃ I ₄ N ₄ O ₄ P ₂ Ru 1604.8 orange-brown, irregula Siemens P4 triclinic, PI 11.744(1) 13.357(1) 20.173(2) 93.19(1) | |
| $\begin{picture}(200,0) \put(0,0){\line(0,0){\mathbb{A}}} \put(0,$ | 0.79 -1.28 12 C ₅₂ H ₄₁ BCl ₂ N ₆ O ₄ Ru ₂ 1097.8 orange, rhombohedron Siemens SMART-CCD triclinic, Pī 10.712(4) 13.939(4) 17.871(7) 67.156(14) 84.40(2) | 0.40 -0.41 Con 14 C ₅₉ H ₄₈ Cl ₂ F ₁₂ N ₁₂ O ₈ P ₂ Ru ₄ 1818.21 orange, equant Siemens SMART-CCD triclinic, PĪ 14.4764(2) 15.0429(2) 17.0034(1) 97.829(1) 106.942(1) | 0.44 -0.36 mpd 15 C ₃₄ H ₂₅ Cl ₂ F ₆ N ₂ O ₄ PRu ₂ 999.6 yellow-brown, lamellar Siemens SMART-CCD orthorhombic, <i>Pbca</i> 17.614(2) 13.624(2) 31.294(2) 90 90 | 0.42 -0.44 16 C _{47.5} H ₃₆ Cl ₃ I ₄ N ₄ O ₄ P ₂ Ru 1604.8 orange-brown, irregula Siemens P ₄ triclinic, P̄I 11.744(1) 13.357(1) 20.173(2) 93.19(1) 95.09(1) | |
| $\begin{picture}(200,0) \put(0,0){\line(0,0){\mathbb{A}}} \put(0,$ | 0.79 -1.28 12 C ₅₂ H ₄₁ BCl ₂ N ₆ O ₄ Ru ₂ 1097.8 orange, rhombohedron Siemens SMART-CCD triclinic, P̄I 10.712(4) 13.939(4) 17.871(7) 67.156(14) 84.40(2) 85.273(16) | 0.40 -0.41 Con 14 C ₅₉ H ₄₈ Cl ₂ F ₁₂ N ₁₂ O ₈ P ₂ Ru ₄ 1818.21 orange, equant Siemens SMART-CCD triclinic, PĪ 14.4764(2) 15.0429(2) 17.0034(1) 97.829(1) 106.942(1) 103.125(1) | 0.44 -0.36 mpd 15 C ₃₄ H ₂₅ Cl ₂ F ₆ N ₂ O ₄ PRu ₂ 999.6 yellow-brown, lamellar Siemens SMART-CCD orthorhombic, <i>Pbca</i> 17.614(2) 13.624(2) 31.294(2) 90 90 90 | 0.42 -0.44 16 C _{47.5} H ₃₆ Cl ₃ I ₄ N ₄ O ₄ P ₂ R ₁ 1604.8 orange-brown, irregulation of the second of the se | |
| $\begin{picture}(200,0) \put(0,0){\line(0,0){\mathbb{A}}} \put(0,$ | 0.79 -1.28 12 C ₅₂ H ₄₁ BCl ₂ N ₆ O ₄ Ru ₂ 1097.8 orange, rhombohedron Siemens SMART-CCD triclinic, P̄I 10.712(4) 13.939(4) 17.871(7) 67.156(14) 84.40(2) 85.273(16) 2444.5(17) | 0.40 -0.41 Con 14 C ₅₉ H ₄₈ Cl ₂ F ₁₂ N ₁₂ O ₈ P ₂ Ru ₄ 1818.21 orange, equant Siemens SMART-CCD triclinic, PĪ 14.4764(2) 15.0429(2) 17.0034(1) 97.829(1) 106.942(1) 103.125(1) 3367.16(7) | 0.44 -0.36 mpd 15 C ₃₄ H ₂₅ Cl ₂ F ₆ N ₂ O ₄ PRu ₂ 999.6 yellow-brown, lamellar Siemens SMART-CCD orthorhombic, <i>Pbca</i> 17.614(2) 13.624(2) 31.294(2) 90 90 90 7509.6(15) | 0.42 -0.44 16 C _{47.5} H ₃₆ Cl ₃ I ₄ N ₄ O ₄ P ₂ Rt 1604.8 orange-brown, irregulated in the second of the sec | |
| (Δρ) _{max} , e Å ⁻³ :(Δρ) _{min} , eÅ ⁻³ (Δρ) _{min} | 0.79 -1.28 12 C ₅₂ H ₄₁ BCl ₂ N ₆ O ₄ Ru ₂ 1097.8 orange, rhombohedron Siemens SMART-CCD triclinic, PĪ 10.712(4) 13.939(4) 17.871(7) 67.156(14) 84.40(2) 85.273(16) 2444.5(17) 2 | 0.40 -0.41 Con 14 C ₅₉ H ₄₈ Cl ₂ F ₁₂ N ₁₂ O ₈ P ₂ Ru ₄ 1818.21 orange, equant Siemens SMART-CCD triclinic, PI 14.4764(2) 15.0429(2) 17.0034(1) 97.829(1) 106.942(1) 103.125(1) 3367.16(7) 2 | 0.44 -0.36 npd 15 C ₃₄ H ₂₅ Cl ₂ F ₆ N ₂ O ₄ PRu ₂ 999.6 yellow-brown, lamellar Siemens SMART-CCD orthorhombic, <i>Pbca</i> 17.614(2) 13.624(2) 31.294(2) 90 90 90 7509.6(15) 8 | 0.42 -0.44 16 C _{47.5} H ₃₆ Cl ₃ I ₄ N ₄ O ₄ P ₂ Rt 1604.8 orange-brown, irregula Siemens P ₄ triclinic, P̄I 11.744(1) 13.357(1) 20.173(2) 93.19(1) 95.09(1) 112.90(1) 2889.3(4) 2 | |
| (Δρ) _{max} , e Å ⁻³ (Δρ) _{min} , eÅ ⁻³ (Δρ) _{min} , | 0.79 -1.28 12 C ₅₂ H ₄₁ BCl ₂ N ₆ O ₄ Ru ₂ 1097.8 orange, rhombohedron Siemens SMART-CCD triclinic, PI 10.712(4) 13.939(4) 17.871(7) 67.156(14) 84.40(2) 85.273(16) 2444.5(17) 2 1.491 | 0.40 -0.41 Con 14 C ₅₉ H ₄₈ Cl ₂ F ₁₂ N ₁₂ O ₈ P ₂ Ru ₄ 1818.21 orange, equant Siemens SMART-CCD triclinic, PI 14.4764(2) 15.0429(2) 17.0034(1) 97.829(1) 106.942(1) 103.125(1) 3367.16(7) 2 1.793 | 0.44 -0.36 Inpd 15 C ₃₄ H ₂₅ Cl ₂ F ₆ N ₂ O ₄ PRu ₂ 999.6 yellow-brown, lamellar Siemens SMART-CCD orthorhombic, <i>Pbca</i> 17.614(2) 13.624(2) 31.294(2) 90 90 90 7509.6(15) 8 1.768 | 0.42 -0.44 T6 C _{47.5} H ₃₆ Cl ₃ I ₄ N ₄ O ₄ P ₂ Ru 1604.8 orange-brown, irregula Siemens P4 triclinic, PI 11.744(1) 13.357(1) 20.173(2) 93.19(1) 95.09(1) 112.90(1) 2889.3(4) 2 1.845 | |
| (Δρ) _{max} , e Å ⁻³ :(Δρ) _{min} , eÅ ⁻³ (Δρ) _{min} | 0.79 -1.28 12 C ₅₂ H ₄₁ BCl ₂ N ₆ O ₄ Ru ₂ 1097.8 orange, rhombohedron Siemens SMART-CCD triclinic, PI 10.712(4) 13.939(4) 17.871(7) 67.156(14) 84.40(2) 85.273(16) 2444.5(17) 2 1.491 0.710 73 | 0.40 -0.41 C ₅₉ H ₄₈ Cl ₂ F ₁₂ N ₁₂ O ₈ P ₂ Ru ₄ 1818.21 orange, equant Siemens SMART-CCD triclinic, Pī 14.4764(2) 15.0429(2) 17.0034(1) 97.829(1) 106.942(1) 103.125(1) 3367.16(7) 2 1.793 0.710 73 | $\begin{array}{c} 0.44\\ -0.36 \\ \\ \hline \\ \textbf{npd} \\ \hline \\ \textbf{C}_{34}\textbf{H}_{25}\textbf{C}\textbf{I}_{2}\textbf{F}_{6}\textbf{N}_{2}\textbf{O}_{4}\textbf{PRu}_{2} \\ 999.6\\ \text{yellow-brown, lamellar} \\ \textbf{Siemens SMART-CCD} \\ \text{orthorhombic, } \textit{Pbca} \\ 17.614(2)\\ 13.624(2)\\ 31.294(2)\\ 90\\ 90\\ 90\\ 7509.6(15)\\ 8\\ 1.768\\ 0.710\ 73 \\ \\ \end{array}$ | 0.42 -0.44 16 C _{47.5} H ₃₆ Cl ₃ I ₄ N ₄ O ₄ P ₂ Ru 1604.8 orange-brown, irregula Siemens P4 triclinic, PI 11.744(1) 13.357(1) 20.173(2) 93.19(1) 95.09(1) 112.90(1) 2889.3(4) 2 1.845 0.710 73 | |
| (Δρ) _{max} , e Å ⁻³ :(Δρ) _{min} , eÅ ⁻³ Enrmula Ex Epolor, habit diffractometer used space group A A C A C A C C C C C C C C C C C C C | 0.79 -1.28 12 C ₅₂ H ₄₁ BCl ₂ N ₆ O ₄ Ru ₂ 1097.8 orange, rhombohedron Siemens SMART-CCD triclinic, PĪ 10.712(4) 13.939(4) 17.871(7) 67.156(14) 84.40(2) 85.273(16) 2444.5(17) 2 1.491 0.710 73 1108 | 0.40 -0.41 Con 14 C ₅₉ H ₄₈ Cl ₂ F ₁₂ N ₁₂ O ₈ P ₂ Ru ₄ 1818.21 orange, equant Siemens SMART-CCD triclinic, PĪ 14.4764(2) 15.0429(2) 17.0034(1) 97.829(1) 106.942(1) 103.125(1) 3367.16(7) 2 1.793 0.710 73 1796 | $\begin{array}{c} 0.44 \\ -0.36 \\ \\ \hline \\ \text{npd} \\ \hline \\ \hline \\ C_{34}\text{H}_{25}\text{Cl}_2\text{F}_6\text{N}_2\text{O}_4\text{PRu}_2 \\ 999.6 \\ \text{yellow-brown, lamellar} \\ \text{Siemens SMART-CCD} \\ \text{orthorhombic, } \textit{Pbca} \\ 17.614(2) \\ 13.624(2) \\ 31.294(2) \\ 90 \\ 90 \\ 90 \\ 7509.6(15) \\ 8 \\ 1.768 \\ 0.710 \ 73 \\ 3952 \\ \end{array}$ | 0.42 -0.44 16 C _{47.5} H ₃₆ Cl ₃ I ₄ N ₄ O ₄ P ₂ Ru 1604.8 orange-brown, irregula Siemens P4 triclinic, PI 11.744(1) 13.357(1) 20.173(2) 93.19(1) 95.09(1) 112.90(1) 2889.3(4) 2 1.845 0.710 73 1524 | |
| $(\Delta \rho)_{\text{max}}$, e Å ⁻³ $(\Delta \rho)_{\text{min}}$, eÅ ⁻³ $(\Delta \rho)_{\text{min}}$, | 0.79 -1.28 12 C ₅₂ H ₄₁ BCl ₂ N ₆ O ₄ Ru ₂ 1097.8 orange, rhombohedron Siemens SMART-CCD triclinic, PĪ 10.712(4) 13.939(4) 17.871(7) 67.156(14) 84.40(2) 85.273(16) 2444.5(17) 2 1.491 0.710 73 1108 whole data | 0.40 -0.41 Con 14 C ₅₉ H ₄₈ Cl ₂ F ₁₂ N ₁₂ O ₈ P ₂ Ru ₄ 1818.21 orange, equant Siemens SMART-CCD triclinic, PĪ 14.4764(2) 15.0429(2) 17.0034(1) 97.829(1) 106.942(1) 103.125(1) 3367.16(7) 2 1.793 0.710 73 1796 whole data | $\begin{array}{c} 0.44 \\ -0.36 \\ \\ \text{npd} \\ \hline \\ \hline C_{34} H_{25} Cl_2 F_6 N_2 O_4 PRu_2 \\ 999.6 \\ \text{yellow-brown, lamellar} \\ \text{Siemens SMART-CCD} \\ \text{orthorhombic, } \textit{Pbca} \\ 17.614(2) \\ 13.624(2) \\ 31.294(2) \\ 90 \\ 90 \\ 90 \\ 90 \\ 7509.6(15) \\ 8 \\ 1.768 \\ 0.710 \ 73 \\ 3952 \\ \text{whole data} \end{array}$ | $\begin{array}{c} \textbf{16} \\ \textbf{C}_{47.5} \textbf{H}_{36} \textbf{C} \textbf{C}_{3} \textbf{I}_{4} \textbf{N}_{4} \textbf{O}_{4} \textbf{P}_{2} \textbf{R}_{1} \\ \textbf{1604.8} \\ \textbf{orange-brown, irregula} \\ \textbf{Siemens P4} \\ \textbf{triclinic, } P \textbf{I} \\ \textbf{11.744(1)} \\ \textbf{13.357(1)} \\ \textbf{20.173(2)} \\ \textbf{93.19(1)} \\ \textbf{95.09(1)} \\ \textbf{112.90(1)} \\ \textbf{2889.3(4)} \\ \textbf{2} \\ \textbf{1.845} \\ \textbf{0.710 73} \\ \textbf{1524} \\ \textbf{25, 24} < 2\theta < 25 \\ \end{array}$ | |
| Aρ) _{max} , e Å ⁻³ (Δρ) _{min} , eÅ ⁻³ (Δρ) _{min} (Δρ) _{min} , eÅ ⁻³ (| 0.79 -1.28 12 C ₅₂ H ₄₁ BCl ₂ N ₆ O ₄ Ru ₂ 1097.8 orange, rhombohedron Siemens SMART-CCD triclinic, Pī 10.712(4) 13.939(4) 17.871(7) 67.156(14) 84.40(2) 85.273(16) 2444.5(17) 2 1.491 0.710 73 1108 whole data hemisphere | 0.40 -0.41 C ₅₉ H ₄₈ Cl ₂ F ₁₂ N ₁₂ O ₈ P ₂ Ru ₄ 1818.21 orange, equant Siemens SMART-CCD triclinic, PĪ 14.4764(2) 15.0429(2) 17.0034(1) 97.829(1) 106.942(1) 103.125(1) 3367.16(7) 2 1.793 0.710 73 1796 whole data hemisphere | 0.44 -0.36 npd 15 C ₃₄ H ₂₅ Cl ₂ F ₆ N ₂ O ₄ PRu ₂ 999.6 yellow-brown, lamellar Siemens SMART-CCD orthorhombic, <i>Pbca</i> 17.614(2) 13.624(2) 31.294(2) 90 90 7509.6(15) 8 1.768 0.710 73 3952 whole data hemisphere | 0.42 -0.44 16 C _{47.5} H ₃₆ Cl ₃ I ₄ N ₄ O ₄ P ₂ R ₁ 1604.8 orange-brown, irregulation of the second of the se | |
| $(\Delta \rho)_{\text{max}}$, e Å ⁻³ $(\Delta \rho)_{\text{min}}$, eÅ ⁻³ $(\Delta \rho)_{\text{min}}$, abit $(\Delta \rho)_{\text{min}}$, $\Delta \rho$ $(\Delta \rho)_{\text{min}}$ | 0.79 -1.28 12 C ₅₂ H ₄₁ BCl ₂ N ₆ O ₄ Ru ₂ 1097.8 orange, rhombohedron Siemens SMART-CCD triclinic, P̄1 10.712(4) 13.939(4) 17.871(7) 67.156(14) 84.40(2) 85.273(16) 2444.5(17) 2 1.491 0.710 73 1108 whole data hemisphere 3-47 | 0.40 -0.41 C ₅₉ H ₄₈ Cl ₂ F ₁₂ N ₁₂ O ₈ P ₂ Ru ₄ 1818.21 orange, equant Siemens SMART-CCD triclinic, PĪ 14.4764(2) 15.0429(2) 17.0034(1) 97.829(1) 106.942(1) 103.125(1) 3367.16(7) 2 1.793 0.710 73 1796 whole data hemisphere 3-51 | 0.44 -0.36 mpd 15 C ₃₄ H ₂₅ Cl ₂ F ₆ N ₂ O ₄ PRu ₂ 999.6 yellow-brown, lamellar Siemens SMART-CCD orthorhombic, <i>Pbca</i> 17.614(2) 13.624(2) 31.294(2) 90 90 7509.6(15) 8 1.768 0.710 73 3952 whole data hemisphere 3-53 | $\begin{array}{c} \textbf{16} \\ \hline \textbf{C}_{47.5} \textbf{H}_{36} \textbf{C} \textbf{I}_{3} \textbf{I}_{4} \textbf{N}_{4} \textbf{O}_{4} \textbf{P}_{2} \textbf{R}_{1} \\ \textbf{1604.8} \\ \textbf{orange-brown, irregular Siemens P4} \\ \textbf{triclinic, } P\overline{\textbf{I}} \\ \textbf{11.744(1)} \\ \textbf{13.357(1)} \\ \textbf{20.173(2)} \\ \textbf{93.19(1)} \\ \textbf{95.09(1)} \\ \textbf{112.90(1)} \\ \textbf{2889.3(4)} \\ \textbf{2} \\ \textbf{1.845} \\ \textbf{0.710 73} \\ \textbf{1524} \\ \textbf{25, 24} < 2\theta < 25 \\ \theta - \omega \\ \textbf{4-45} \\ \end{array}$ | |
| $\Box (\Delta \rho)_{\text{max}}$, e Å ⁻³ \vdots $(\Delta \rho)_{\text{min}}$, eÅ ⁻³ \vdots $(\Delta \rho)_{m$ | $\begin{array}{c} 0.79 \\ -1.28 \\ \hline \\ \hline & 12 \\ \hline \\ \hline & 12 \\ \hline \\ \hline & 197.8 \\ orange, rhombohedron \\ Siemens SMART-CCD \\ triclinic, P\overline{1} \\ 10.712(4) \\ 13.939(4) \\ 17.871(7) \\ 67.156(14) \\ 84.40(2) \\ 85.273(16) \\ 2444.5(17) \\ 2 \\ 1.491 \\ 0.710 \ 73 \\ 1108 \\ \text{whole data hemisphere} \\ 3-47 \\ \pm 11, \pm 15, 19 \\ \hline \end{array}$ | $\begin{array}{c} 0.40 \\ -0.41 \\ \hline \\ \hline \textbf{14} \\ \hline \\ C_{59}H_{48}Cl_2F_{12}N_{12}O_8P_2Ru_4 \\ 1818.21 \\ \text{orange, equant} \\ \text{Siemens SMART-CCD} \\ \text{triclinic, } \overrightarrow{P1} \\ 14.4764(2) \\ 15.0429(2) \\ 17.0034(1) \\ 97.829(1) \\ 106.942(1) \\ 103.125(1) \\ 3367.16(7) \\ 2 \\ 1.793 \\ 0.710\ 73 \\ 1796 \\ \text{whole data} \\ \text{hemisphere} \\ 3-51 \\ \pm 17, \pm 17, 20 \\ \hline \end{array}$ | 0.44 -0.36 npd 15 C ₃₄ H ₂₅ Cl ₂ F ₆ N ₂ O ₄ PRu ₂ 999.6 yellow-brown, lamellar Siemens SMART-CCD orthorhombic, <i>Pbca</i> 17.614(2) 13.624(2) 31.294(2) 90 90 7509.6(15) 8 1.768 0.710 73 3952 whole data hemisphere 3-53 20,16,36 | $\begin{array}{c} \textbf{16} \\ \hline \textbf{C}_{47.5} \textbf{H}_{36} \textbf{C} \textbf{I}_{3} \textbf{I}_{4} \textbf{N}_{4} \textbf{O}_{4} \textbf{P}_{2} \textbf{R}_{1} \\ \textbf{1604.8} \\ \textbf{orange-brown, irregular Siemens P4} \\ \textbf{triclinic, } P\overline{\textbf{I}} \\ \textbf{11.744(1)} \\ \textbf{13.357(1)} \\ \textbf{20.173(2)} \\ \textbf{93.19(1)} \\ \textbf{95.09(1)} \\ \textbf{112.90(1)} \\ \textbf{2889.3(4)} \\ \textbf{2} \\ \textbf{1.845} \\ \textbf{0.710 73} \\ \textbf{1524} \\ \textbf{25, 24} < 2\theta < 25 \\ \theta - \omega \\ \textbf{4-45} \\ \textbf{12,\pm 14,\pm 21} \\ \end{array}$ | |
| $\Xi(\Delta\rho)_{\text{min}}$, eÅ ⁻³ $\Xi(\Delta\rho)_{\text{min}}$, deg $\Xi(\Delta\rho)_{\text{min}}$, deg $\Xi(\Delta\rho)_{\text{min}}$, deg $\Xi(\Delta\rho)_{\text{min}}$, eÅ ⁻³ $\Xi(\Delta\rho)_{\text{min}}$, deg $\Xi(\Delta\rho)_{\text{min}}$, eÅ ⁻³ $\Xi(\Delta\rho)_{\text{min}}$, deg $\Xi(\Delta\rho)_{\text{min}}$, eÅ ⁻³ $\Xi(\Delta\rho)_{\text{min}}$, eÅ ⁻³ $\Xi(\Delta\rho)_{\text{min}}$, deg $\Xi(\Delta\rho)_{\text{min}}$, eÅ ⁻³ $\Xi(\Delta\rho)_{mi$ | 0.79 -1.28 -1.28 -1.28 -1.28 -1.28 -1.28 -1.28 -1.28 -1.28 -1.29 -1.28 -1.29 -1.28 -1.20 -1.2 | 0.40 -0.41 C ₅₉ H ₄₈ Cl ₂ F ₁₂ N ₁₂ O ₈ P ₂ Ru ₄ 1818.21 orange, equant Siemens SMART-CCD triclinic, PĪ 14.4764(2) 15.0429(2) 17.0034(1) 97.829(1) 106.942(1) 103.125(1) 3367.16(7) 2 1.793 0.710 73 1796 whole data hemisphere 3-51 ±17,±17,20 11.02 | 0.44 -0.36 npd 15 C ₃₄ H ₂₅ Cl ₂ F ₆ N ₂ O ₄ PRu ₂ 999.6 yellow-brown, lamellar Siemens SMART-CCD orthorhombic, <i>Pbca</i> 17.614(2) 13.624(2) 31.294(2) 90 90 7509.6(15) 8 1.768 0.710 73 3952 whole data hemisphere 3-53 20,16,36 10.66 | $\begin{array}{c} \textbf{16} \\ \hline \textbf{C}_{47.5} \textbf{H}_{36} \textbf{C} \textbf{I}_{3} \textbf{I}_{4} \textbf{N}_{4} \textbf{O}_{4} \textbf{P}_{2} \textbf{R}_{1} \\ \textbf{1604.8} \\ \textbf{orange-brown, irregular Siemens P4} \\ \textbf{triclinic, } P\overline{\textbf{I}} \\ \textbf{11.744(1)} \\ \textbf{13.357(1)} \\ \textbf{20.173(2)} \\ \textbf{93.19(1)} \\ \textbf{95.09(1)} \\ \textbf{112.90(1)} \\ \textbf{2889.3(4)} \\ \textbf{2} \\ \textbf{1.845} \\ \textbf{0.710 73} \\ \textbf{1524} \\ \textbf{25, } \textbf{24} < \textbf{2}\theta < \textbf{25} \\ \theta - \omega \\ \textbf{4-45} \\ \textbf{12,\pm 14,\pm 21} \\ \textbf{28.96} \\ \end{array}$ | |
| $\Box(\Delta\rho)_{\text{max}}$, e Å ⁻³ $\vdots(\Delta\rho)_{\text{min}}$, eÅ ⁻³ $\vdots(\Delta\rho)_{\text{min}}$, deg $\vdots(\Delta\rho)_{\text{min}}$, deg $\vdots(\Delta\rho)_{\text{min}}$, deg $\vdots(\Delta\rho)_{\text{min}}$, deg $\vdots(\Delta\rho)_{\text{min}}$, eÅ ⁻³ $\vdots(\Delta\rho)_{\text{min}}$, deg $\vdots(\Delta\rho)_{\text{min}}$, deg $\vdots(\Delta\rho)_{\text{min}}$, eÅ ⁻³ $\vdots(\Delta\rho)_{m$ | $\begin{array}{c} 0.79 \\ -1.28 \\ \hline \\ \hline 12 \\ \hline \\ C_{52}H_{41}BCl_2N_6O_4Ru_2 \\ 1097.8 \\ orange, rhombohedron \\ Siemens SMART-CCD \\ triclinic, P\overline{1} \\ 10.712(4) \\ 13.939(4) \\ 17.871(7) \\ 67.156(14) \\ 84.40(2) \\ 85.273(16) \\ 2444.5(17) \\ 2 \\ 1.491 \\ 0.710 \ 73 \\ 1108 \\ \text{whole data hemisphere} \\ 3-47 \\ \pm 11,\pm 15,19 \\ 7.78 \\ 0.3 \times 0.3 \times 0.4 \\ \hline \end{array}$ | 0.40 -0.41 C ₅₉ H ₄₈ Cl ₂ F ₁₂ N ₁₂ O ₈ P ₂ Ru ₄ 1818.21 orange, equant Siemens SMART-CCD triclinic, PI 14.4764(2) 15.0429(2) 17.0034(1) 97.829(1) 106.942(1) 103.125(1) 3367.16(7) 2 1.793 0.710 73 1796 whole data hemisphere 3-51 ±17,±17,20 11.02 0.48 × 0.45 × 0.38 | $\begin{array}{c} 0.44 \\ -0.36 \\ \\ \hline \\ \text{npd} \\ \hline \\ \hline \\ C_{34}\text{H}_{25}\text{Cl}_2\text{F}_6\text{N}_2\text{O}_4\text{PRu}_2 \\ 999.6 \\ \text{yellow-brown, lamellar} \\ \text{Siemens SMART-CCD} \\ \text{orthorhombic, } \textit{Pbca} \\ 17.614(2) \\ 13.624(2) \\ 31.294(2) \\ 90 \\ 90 \\ \\ 7509.6(15) \\ 8 \\ 1.768 \\ 0.710 \ 73 \\ 3952 \\ \text{whole data} \\ \text{hemisphere} \\ 3-53 \\ 20.16,36 \\ 10.66 \\ 0.61 \times 0.46 \times 0.08 \\ \\ \end{array}$ | $\begin{array}{c} \textbf{16} \\ \textbf{C}_{47.5}\textbf{H}_{36}\textbf{Cl}_{3}\textbf{I}_{4}\textbf{N}_{4}\textbf{O}_{4}\textbf{P}_{2}\textbf{R}_{1} \\ \textbf{1604.8} \\ \textbf{orange-brown, irregula} \\ \textbf{Siemens P4} \\ \textbf{triclinic, } P\textbf{I} \\ \textbf{11.744(1)} \\ \textbf{13.357(1)} \\ \textbf{20.173(2)} \\ \textbf{93.19(1)} \\ \textbf{95.09(1)} \\ \textbf{112.90(1)} \\ \textbf{2889.3(4)} \\ \textbf{2} \\ \textbf{1.845} \\ \textbf{0.710 73} \\ \textbf{1524} \\ \textbf{25, 24} < 2\theta < 25 \\ \theta - \omega \\ \textbf{4-45} \\ \textbf{12.\pm 14.\pm 21} \\ \textbf{28.96} \\ \textbf{0.15} \times \textbf{0.3} \times \textbf{0.4} \\ \end{array}$ | |
| $(\Delta \rho)_{\text{max}}$, e Å ⁻³ $(\Delta \rho)_{\text{min}}$, eÅ ⁻³ $(\Delta \rho)_{\text{min}}$, deg $(\Delta \rho)_{\text{min}}$, eÅ ⁻³ $(\Delta \rho)_{\text{min}}$, deg $(\Delta \rho)_{\text{min}}$, deg $(\Delta \rho)_{\text{min}}$, deg $(\Delta \rho)_{\text{min}}$, eÅ ⁻³ $(\Delta \rho)_{\text{min}}$, eÅ | 0.79 -1.28 12 C ₅₂ H ₄₁ BCl ₂ N ₆ O ₄ Ru ₂ 1097.8 orange, rhombohedron Siemens SMART-CCD triclinic, PĪ 10.712(4) 13.939(4) 17.871(7) 67.156(14) 84.40(2) 85.273(16) 2444.5(17) 2 1.491 0.710 73 1108 whole data hemisphere 3-47 ±11,±15,19 7.78 0.3 × 0.3 × 0.4 298 | 0.40 -0.41 Con 14 C ₅₉ H ₄₈ Cl ₂ F ₁₂ N ₁₂ O ₈ P ₂ Ru ₄ 1818.21 orange, equant Siemens SMART-CCD triclinic, $P\bar{1}$ 14.4764(2) 15.0429(2) 17.0034(1) 97.829(1) 106.942(1) 103.125(1) 3367.16(7) 2 1.793 0.710 73 1796 whole data hemisphere 3-51 \pm 17, \pm 17, \pm 17,20 11.02 0.48 × 0.45 × 0.38 296 | $\begin{array}{c} 0.44 \\ -0.36 \\ \\ \hline \\ \text{npd} \\ \hline \\ \hline \\ C_{34}\text{H}_{25}\text{Cl}_2\text{F}_6\text{N}_2\text{O}_4\text{PRu}_2 \\ 999.6 \\ \text{yellow-brown, lamellar} \\ \text{Siemens SMART-CCD} \\ \text{orthorhombic, } \textit{Pbca} \\ 17.614(2) \\ 13.624(2) \\ 31.294(2) \\ 90 \\ 90 \\ 90 \\ \\ 90 \\ \\ 90 \\ \\ 90 \\ \\ 509.6(15) \\ 8 \\ 0.710 \ 73 \\ 3952 \\ \text{whole data} \\ \text{hemisphere} \\ 3-53 \\ 20.16.36 \\ 10.66 \\ 0.61 \times 0.46 \times 0.08 \\ 296 \\ \end{array}$ | $\begin{array}{c} \textbf{16} \\ \textbf{C}_{47.5} \textbf{H}_{36} \textbf{C}_{13} \textbf{I}_{4} \textbf{N}_{4} \textbf{O}_{4} \textbf{P}_{2} \textbf{R} \textbf{I}_{1604.8} \\ \textbf{orange-brown, irregularization, } P\textbf{I} \\ \textbf{11.744} \textbf{(1)} \\ \textbf{13.357} \textbf{(1)} \\ \textbf{20.173} \textbf{(2)} \\ \textbf{93.19} \textbf{(1)} \\ \textbf{95.09} \textbf{(1)} \\ \textbf{112.90} \textbf{(1)} \\ \textbf{2889.3} \textbf{(4)} \\ \textbf{2} \\ \textbf{1.845} \\ \textbf{0.710} \textbf{ 73} \\ \textbf{1524} \\ \textbf{25, 24} < 2\theta < 25 \\ \theta - \omega \\ \textbf{4-45} \\ \textbf{12,\pm 14,\pm 21} \\ \textbf{28.96} \\ \textbf{0.15} \times \textbf{0.3} \times \textbf{0.4} \\ \textbf{298} \\ \end{array}$ | |
| $(\Delta \rho)_{\text{max}}$, e Å ⁻³ $(\Delta \rho)_{\text{min}}$, eÅ ⁻³ $(\Delta \rho)_{\text{min}}$, deg $(\Delta \rho)_{\text{min}}$, eÅ ⁻³ $(\Delta \rho)_{\text{min}}$, deg $(\Delta \rho)_{\text{min}}$, eÅ ⁻³ $(\Delta \rho)_{m$ | 0.79 -1.28 12 C ₅₂ H ₄₁ BCl ₂ N ₆ O ₄ Ru ₂ 1097.8 orange, rhombohedron Siemens SMART-CCD triclinic, PĪ 10.712(4) 13.939(4) 17.871(7) 67.156(14) 84.40(2) 85.273(16) 2444.5(17) 2 1.491 0.710 73 1108 whole data hemisphere 3-47 ±11,±15,19 7.78 0.3 × 0.3 × 0.4 298 9549 | 0.40 -0.41 Con 14 C ₅₉ H ₄₈ Cl ₂ F ₁₂ N ₁₂ O ₈ P ₂ Ru ₄ 1818.21 orange, equant Siemens SMART-CCD triclinic, $P\bar{1}$ 14.4764(2) 15.0429(2) 17.0034(1) 97.829(1) 106.942(1) 103.125(1) 3367.16(7) 2 1.793 0.710 73 1796 whole data hemisphere 3-51 \pm 17, \pm 17, \pm 17,20 11.02 0.48 × 0.45 × 0.38 296 19 376 | $\begin{array}{c} 0.44 \\ -0.36 \\ \\ \hline \\ \text{npd} \\ \hline \\ \hline \\ C_{34}\text{H}_{25}\text{Cl}_2\text{F}_6\text{N}_2\text{O}_4\text{PRu}_2 \\ 999.6 \\ \text{yellow-brown, lamellar} \\ \text{Siemens SMART-CCD} \\ \text{orthorhombic, } \textit{Pbca} \\ 17.614(2) \\ 13.624(2) \\ 31.294(2) \\ 90 \\ 90 \\ 90 \\ 90 \\ \\ 90 \\ 90 \\ \\ 509.6(15) \\ 8 \\ 1.768 \\ 0.710 \ 73 \\ 3952 \\ \text{whole data} \\ \text{hemisphere} \\ 3-53 \\ 20.16.36 \\ 10.66 \\ 0.61 \times 0.46 \times 0.08 \\ 296 \\ 32 \ 873 \\ \hline \end{array}$ | 0.42 -0.44 16 C _{47.5} H ₃₆ Cl ₃ I ₄ N ₄ O ₄ P ₂ Ru 1604.8 orange-brown, irregula Siemens P4 triclinic, PI 11.744(1) 13.357(1) 20.173(2) 93.19(1) 95.09(1) 112.90(1) 2889.3(4) 2 1.845 0.710 73 1524 25, 24 < 2 θ < 25 θ - ω 4-45 12, \pm 14, \pm 21 28.96 0.15 × 0.3 × 0.4 298 7994 | |
| $(\Delta \rho)_{\text{max}}$, e Å ⁻³ $(\Delta \rho)_{\text{min}}$, eÅ ⁻³ $(\Delta \rho)_{\text{min}}$, | $\begin{array}{c} 0.79 \\ -1.28 \\ \hline \\ \hline 12 \\ \hline \\ C_{52}H_{41}BCl_2N_6O_4Ru_2 \\ 1097.8 \\ orange, rhombohedron \\ Siemens SMART-CCD \\ triclinic, P\overline{1} \\ 10.712(4) \\ 13.939(4) \\ 17.871(7) \\ 67.156(14) \\ 84.40(2) \\ 85.273(16) \\ 2444.5(17) \\ 2 \\ 1.491 \\ 0.710.73 \\ 1108 \\ whole data \\ hemisphere \\ 3-47 \\ \pm 11,\pm 15,19 \\ 7.78 \\ 0.3 \times 0.3 \times 0.4 \\ 298 \\ 9549 \\ 6877 \\ \hline \end{array}$ | 0.40 -0.41 Con 14 C ₅₉ H ₄₈ Cl ₂ F ₁₂ N ₁₂ O ₈ P ₂ Ru ₄ 1818.21 orange, equant Siemens SMART-CCD triclinic, $P\bar{1}$ 14.4764(2) 15.0429(2) 17.0034(1) 97.829(1) 106.942(1) 103.125(1) 3367.16(7) 2 1.793 0.710 73 1796 whole data hemisphere 3-51 \pm 17, \pm 17, \pm 20 11.02 0.48 × 0.45 × 0.38 296 19 376 11 036 | $\begin{array}{c} 0.44\\ -0.36\\ \\ \hline \\ npd\\ \hline \\ \hline \\ C_{34}H_{25}Cl_2F_6N_2O_4PRu_2\\ 999.6\\ \\ yellow-brown, lamellar\\ Siemens SMART-CCD\\ orthorhombic, Pbca\\ 17.614(2)\\ 13.624(2)\\ 31.294(2)\\ 90\\ 90\\ 90\\ 7509.6(15)\\ 8\\ 1.768\\ 0.710\ 73\\ 3952\\ whole data\\ hemisphere\\ 3-53\\ 20.16,36\\ 10.66\\ 0.61\times0.46\times0.08\\ 296\\ 32\ 873\\ 6756\\ \end{array}$ | $\begin{array}{c} \textbf{16} \\ \hline \textbf{C}_{47.5} \textbf{H}_{36} \textbf{C} \textbf{C}_{3} \textbf{I}_{4} \textbf{N}_{4} \textbf{O}_{4} \textbf{P}_{2} \textbf{R}_{1} \\ \textbf{1604.8} \\ \textbf{orange-brown, irregul:} \\ \textbf{Siemens P4} \\ \textbf{triclinic, } P \textbf{I} \\ \textbf{11.744(1)} \\ \textbf{13.357(1)} \\ \textbf{20.173(2)} \\ \textbf{93.19(1)} \\ \textbf{95.09(1)} \\ \textbf{112.90(1)} \\ \textbf{2889.3(4)} \\ \textbf{2} \\ \textbf{1.845} \\ \textbf{0.710 73} \\ \textbf{1524} \\ \textbf{25, 24 < 2} \theta < \textbf{25} \\ \theta - \omega \\ \textbf{4-45} \\ \textbf{12, \pm 14, \pm 21} \\ \textbf{28.96} \\ \textbf{0.15 \times 0.3 \times 0.4} \\ \textbf{298} \\ \textbf{7994} \\ \textbf{7546} \\ \end{array}$ | |
| Ξ(Δρ) _{max} , e Å ⁻³ (Δρ) _{min} , eÅ ⁻³ (Δρ) | $\begin{array}{c} 0.79 \\ -1.28 \\ \hline \\ \hline 12 \\ \hline \\ C_{52}H_{41}BCl_2N_6O_4Ru_2 \\ 1097.8 \\ orange, rhombohedron \\ Siemens SMART-CCD \\ triclinic, $P\overline{1}$ \\ 10.712(4) \\ 13.939(4) \\ 17.871(7) \\ 67.156(14) \\ 84.40(2) \\ 85.273(16) \\ 2444.5(17) \\ 2 \\ 1.491 \\ 0.710.73 \\ 1108 \\ whole data \\ hemisphere \\ 3-47 \\ \pm 11,\pm 15,19 \\ 7.78 \\ 0.3 \times 0.3 \times 0.4 \\ 298 \\ 9549 \\ 6877 \\ 5837 (>4\sigma) \\ \end{array}$ | 0.40 -0.41 Con 14 C ₅₉ H ₄₈ Cl ₂ F ₁₂ N ₁₂ O ₈ P ₂ Ru ₄ 1818.21 orange, equant Siemens SMART-CCD triclinic, $P\bar{1}$ 14.4764(2) 15.0429(2) 17.0034(1) 97.829(1) 106.942(1) 103.125(1) 3367.16(7) 2 1.793 0.710 73 1796 whole data hemisphere 3-51 \pm 17, \pm 17, \pm 20 11.02 0.48 × 0.45 × 0.38 296 19 376 11 036 11033 (>2 σ) | $\begin{array}{c} 0.44\\ -0.36\\ \\ \hline \\ npd\\ \hline \\ \hline \\ C_{34}H_{25}Cl_2F_6N_2O_4PRu_2\\ 999.6\\ \\ yellow-brown, lamellar\\ Siemens SMART-CCD\\ orthorhombic, Pbca\\ 17.614(2)\\ 13.624(2)\\ 31.294(2)\\ 90\\ 90\\ 90\\ 7509.6(15)\\ 8\\ 1.768\\ 0.710\\ 73\\ 3952\\ whole data\\ hemisphere\\ 3-53\\ 20.16,36\\ 10.66\\ 0.61\times0.46\times0.08\\ 296\\ 32\\ 873\\ 6756\\ 4934\ (>3\sigma)\\ \end{array}$ | 0.42 -0.44 16 C _{47.5} H ₃₆ Cl ₃ I ₄ N ₄ O ₄ P ₂ R ₁ 1604.8 orange-brown, irregulation of the constant of | |
| $\Box(\Delta\rho)_{\text{max}}$, e Å ⁻³ \vdots $(\Delta\rho)_{\text{min}}$, eÅ ⁻³ \vdots | $\begin{array}{c} 0.79 \\ -1.28 \\ \hline \\ \hline & 12 \\ \hline \\ \hline & 12 \\ \hline \\ \hline & 12 \\ \hline \\ \hline & 1097.8 \\ \text{orange, rhombohedron} \\ \text{Siemens SMART-CCD} \\ \text{triclinic, } P\overline{1} \\ 10.712(4) \\ 13.939(4) \\ 17.871(7) \\ 67.156(14) \\ 84.40(2) \\ 85.273(16) \\ 2444.5(17) \\ 2 \\ 1.491 \\ 0.710.73 \\ 1108 \\ \text{whole data hemisphere} \\ 3-47 \\ \pm 11, \pm 15, 19 \\ 7.78 \\ 0.3 \times 0.3 \times 0.4 \\ 298 \\ 9549 \\ 6877 \\ 5837 (> 4\sigma) \\ 0.055, 0.068 \\ \hline \end{array}$ | 0.40 -0.41 Con 14 C ₅₉ H ₄₈ Cl ₂ F ₁₂ N ₁₂ O ₈ P ₂ Ru ₄ 1818.21 orange, equant Siemens SMART-CCD triclinic, $P\bar{1}$ 14.4764(2) 15.0429(2) 17.0034(1) 97.829(1) 106.942(1) 103.125(1) 3367.16(7) 2 1.793 0.710 73 1796 whole data hemisphere 3-51 \pm 17, \pm 17, \pm 17,20 11.02 0.48 × 0.45 × 0.38 296 19 376 11 036 11 036 11033 (>2 σ) 0.040, 0.051 | 0.44 -0.36 npd 15 C ₃₄ H ₂₅ Cl ₂ F ₆ N ₂ O ₄ PRu ₂ 999.6 yellow-brown, lamellar Siemens SMART-CCD orthorhombic, <i>Pbca</i> 17.614(2) 13.624(2) 31.294(2) 90 90 7509.6(15) 8 1.768 0.710 73 3952 whole data hemisphere 3-53 20,16,36 10.66 0.61 × 0.46 × 0.08 296 32 873 6756 4934 (>3\sigma) 0.047, 0.051 | 0.42 -0.44 16 C _{47.5} H ₃₆ Cl ₃ I ₄ N ₄ O ₄ P ₂ R ₁ 1604.8 orange-brown, irregulation of the properties of the prop | |
| $\Box(\Delta\rho)_{\text{max}}$, e Å ⁻³ $\vdots(\Delta\rho)_{\text{min}}$, eÅ ⁻³ $\vdots(\Delta\rho)_{\text{min}}$, deg $\vdots(\Delta\rho)_{\text{min}}$, eÅ ⁻³ $\vdots(\Delta\rho)_{min$ | $\begin{array}{c} 0.79 \\ -1.28 \\ \hline \\ \hline & 12 \\ \hline \\ \hline & 12 \\ \hline \\ \hline & 1097.8 \\ orange, rhombohedron \\ Siemens SMART-CCD \\ triclinic, P\overline{1} \\ 10.712(4) \\ 13.939(4) \\ 17.871(7) \\ 67.156(14) \\ 84.40(2) \\ 85.273(16) \\ 2444.5(17) \\ 2 \\ 1.491 \\ 0.710 \ 73 \\ 1108 \\ \text{whole data hemisphere } \\ 3-47 \\ \pm 11,\pm 15,19 \\ 7.78 \\ 0.3 \times 0.3 \times 0.4 \\ 298 \\ 9549 \\ 6877 \\ 5837 \ (>4\sigma) \\ 0.055, 0.068 \\ 1.89 \\ \hline \end{array}$ | 0.40 -0.41 Con 14 C ₅₉ H ₄₈ Cl ₂ F ₁₂ N ₁₂ O ₈ P ₂ Ru ₄ 1818.21 orange, equant Siemens SMART-CCD triclinic, $P\bar{1}$ 14.4764(2) 15.0429(2) 17.0034(1) 97.829(1) 106.942(1) 103.125(1) 3367.16(7) 2 1.793 0.710 73 1796 whole data hemisphere 3-51 $\pm 17, \pm 17, \pm 20$ 11.02 0.48 × 0.45 × 0.38 296 19 376 11 036 11 036 11 036 11033 (> 2 σ) 0.040, 0.051 1.09 | $\begin{array}{c} 0.44\\ -0.36\\ \\ \hline \\ npd\\ \hline \\ \hline \\ C_{34}H_{25}Cl_2F_6N_2O_4PRu_2\\ 999.6\\ \\ yellow-brown, lamellar\\ Siemens SMART-CCD\\ orthorhombic, Pbca\\ 17.614(2)\\ 13.624(2)\\ 31.294(2)\\ 90\\ 90\\ \\ 7509.6(15)\\ 8\\ 1.768\\ 0.710\\ 73\\ 3952\\ \\ whole data\\ hemisphere\\ 3-53\\ 20.16.36\\ 10.66\\ 0.61\\ \times 0.46\\ \times 0.08\\ 296\\ 32\\ 873\\ 6756\\ 4934\\ (>3\sigma)\\ 0.047, 0.051\\ 1.34\\ \hline \end{array}$ | 0.42 -0.44 16 C _{47.5} H ₃₆ Cl ₃ I ₄ N ₄ O ₄ P ₂ R ₁ 1604.8 orange-brown, irregulation of the properties of the prop | |
| $\square(\Delta\rho)_{\text{max}}$, e Å ⁻³ $\square(\Delta\rho)_{\text{min}}$, eÅ ⁻³ $\square(\Delta\rho)_{\text{min}}$, deg $\square(\Delta\rho)_{\text{min}}$, eÅ ⁻³ $\square($ | $\begin{array}{c} 0.79 \\ -1.28 \\ \hline \\ \hline 12 \\ \hline \\ C_{52}H_{41}BCl_2N_6O_4Ru_2 \\ 1097.8 \\ orange, rhombohedron \\ Siemens SMART-CCD \\ triclinic, P\overline{1} \\ 10.712(4) \\ 13.939(4) \\ 17.871(7) \\ 67.156(14) \\ 84.40(2) \\ 85.273(16) \\ 2444.5(17) \\ 2 \\ 1.491 \\ 0.710 \ 73 \\ 1108 \\ \text{whole data hemisphere} \\ 3-47 \\ \pm 11,\pm 15,19 \\ 7.78 \\ 0.3 \times 0.3 \times 0.4 \\ 298 \\ 9549 \\ 6877 \\ 5837 \ (>4\sigma) \\ 0.055, 0.068 \\ 1.89 \\ \text{SHELXTL-PLUS} \\ \hline \end{array}$ | 0.40 -0.41 Con 14 C ₅₉ H ₄₈ Cl ₂ F ₁₂ N ₁₂ O ₈ P ₂ Ru ₄ 1818.21 orange, equant Siemens SMART-CCD triclinic, $P\bar{1}$ 14.4764(2) 15.0429(2) 17.0034(1) 97.829(1) 106.942(1) 103.125(1) 3367.16(7) 2 1.793 0.710 73 1796 whole data hemisphere 3-51 $\pm 17,\pm 17,20$ 11.02 0.48 × 0.45 × 0.38 296 19 376 11 036 11 036 11 036 11 036 11 037 11.09 SHELXTL-PLUS | $\begin{array}{c} 0.44 \\ -0.36 \\ \\ \hline \\ \text{npd} \\ \hline \\ \hline \\ C_{34}\text{H}_{25}\text{Cl}_2\text{F}_6\text{N}_2\text{O}_4\text{PRu}_2 \\ 999.6 \\ \text{yellow-brown, lamellar} \\ \text{Siemens SMART-CCD} \\ \text{orthorhombic, } \textit{Pbca} \\ 17.614(2) \\ 13.624(2) \\ 31.294(2) \\ 90 \\ 90 \\ 90 \\ 90 \\ \\ 90 \\ \\ 90 \\ \\ 90 \\ \\ 90 \\ \\ 90 \\ \\ 90 \\ \\ 90 \\ \\ 30.7509.6(15) \\ 8 \\ 1.768 \\ 0.710.73 \\ 3952 \\ \text{whole data hemisphere} \\ 3-53 \\ 20.16,36 \\ 10.66 \\ 0.61 \times 0.46 \times 0.08 \\ 296 \\ 32.873 \\ 6756 \\ 4934 \ (>3\sigma) \\ 0.047, 0.051 \\ 1.34 \\ \text{SHELXTL-PLUS} \\ \end{array}$ | 0.42 -0.44 16 $C_{47.5}H_{36}Cl_3I_4N_4O_4P_2R_1$ 1604.8 orange-brown, irregula Siemens P4 triclinic, $P\bar{1}$ 11.744(1) 13.357(1) 20.173(2) 93.19(1) 95.09(1) 112.90(1) 2889.3(4) 2 1.845 0.710 73 1524 25, 24 < 2 θ < 25 θ - ω 4-45 12, \pm 14, \pm 21 28.96 0.15 × 0.3 × 0.4 298 7994 7546 4260 (>6 σ) 0.048, 0.057 1.61 SHELXTL-PLUS | |
| $(Δρ)_{max}$, e Å ⁻³ $(Δρ)_{min}$, eÅ ⁻³ $(Δρ)_$ | $\begin{array}{c} 0.79 \\ -1.28 \\ \hline \\ \hline 12 \\ \hline \\ C_{52}H_{41}BCl_2N_6O_4Ru_2 \\ 1097.8 \\ orange, rhombohedron \\ Siemens SMART-CCD \\ triclinic, P\bar{1} \\ 10.712(4) \\ 13.939(4) \\ 17.871(7) \\ 67.156(14) \\ 84.40(2) \\ 85.273(16) \\ 2444.5(17) \\ 2 \\ 1.491 \\ 0.710 \ 73 \\ 1108 \\ \text{whole data hemisphere } \\ 3-47 \\ \pm 11,\pm 15,19 \\ 7.78 \\ 0.3 \times 0.3 \times 0.4 \\ 298 \\ 9549 \\ 6877 \\ 5837 \ (>4\sigma) \\ 0.055, \ 0.068 \\ 1.89 \\ SHELXTL-PLUS \\ 556 \\ \hline \end{array}$ | 0.40 -0.41 Con 14 C ₅₉ H ₄₈ Cl ₂ F ₁₂ N ₁₂ O ₈ P ₂ Ru ₄ 1818.21 orange, equant Siemens SMART-CCD triclinic, $P\bar{1}$ 14.4764(2) 15.0429(2) 17.0034(1) 97.829(1) 106.942(1) 103.125(1) 3367.16(7) 2 1.793 0.710 73 1796 whole data hemisphere 3-51 \pm 17, \pm 17, \pm 17,20 11.02 0.48 × 0.45 × 0.38 296 19 376 11 036 11033 (>2 σ) 0.040, 0.051 1.09 SHELXTL-PLUS | $\begin{array}{c} 0.44 \\ -0.36 \\ \\ \hline \\ \text{npd} \\ \hline \\ \hline \\ C_{34}\text{H}_{25}\text{Cl}_2\text{F}_6\text{N}_2\text{O}_4\text{PRu}_2 \\ 999.6 \\ \text{yellow-brown, lamellar} \\ \text{Siemens SMART-CCD} \\ \text{orthorhombic, } \textit{Pbca} \\ 17.614(2) \\ 13.624(2) \\ 31.294(2) \\ 90 \\ 90 \\ 90 \\ 90 \\ \\ 90 \\ 90 \\ \\ 7509.6(15) \\ 8 \\ 1.768 \\ 0.710 \ 73 \\ 3952 \\ \text{whole data} \\ \text{hemisphere} \\ 3-53 \\ 20.16.36 \\ 10.66 \\ 0.61 \times 0.46 \times 0.08 \\ 296 \\ 32 \ 873 \\ 6756 \\ 4934 \ (>3\sigma) \\ 0.047, 0.051 \\ 1.34 \\ \text{SHELXTL-PLUS} \\ 497 \\ \end{array}$ | $\begin{array}{c} \textbf{16} \\ \textbf{C}_{47.5} \textbf{H}_{36} \textbf{C}_{13} \textbf{I}_{4} \textbf{N}_{4} \textbf{O}_{4} \textbf{P}_{2} \textbf{R}_{4} \\ \textbf{1604.8} \\ \textbf{orange-brown, irregula} \\ \textbf{Siemens P4} \\ \textbf{triclinic, } P\textbf{I} \\ \textbf{11.744(1)} \\ \textbf{13.357(1)} \\ \textbf{20.173(2)} \\ \textbf{93.19(1)} \\ \textbf{95.09(1)} \\ \textbf{112.90(1)} \\ \textbf{2889.3(4)} \\ \textbf{2} \\ \textbf{1.845} \\ \textbf{0.710 73} \\ \textbf{1524} \\ \textbf{25, 24} < 2\theta < 25 \\ \theta - \omega \\ \textbf{4-45} \\ \textbf{12,\pm 14,\pm 21} \\ \textbf{28.96} \\ \textbf{0.15} \times \textbf{0.3} \times \textbf{0.4} \\ \textbf{298} \\ \textbf{7994} \\ \textbf{7546} \\ \textbf{4260} \ (>6\sigma) \\ \textbf{0.048, 0.057} \\ \textbf{1.61} \\ \textbf{SHELXTL-PLUS} \\ \textbf{429} \\ \end{array}$ | |
| $(\Delta \rho)_{\text{max}}$, e Å ⁻³ $(\Delta \rho)_{\text{min}}$, eÅ ⁻³ $(\Delta \rho)_{\text{min}}$, | $\begin{array}{c} 0.79 \\ -1.28 \\ \hline \\ \textbf{12} \\ \hline \\ \textbf{C}_{52}H_{41}BCl_2N_6O_4Ru_2 \\ 1097.8 \\ \text{orange, rhombohedron} \\ \text{Siemens SMART-CCD} \\ \text{triclinic, } P\overline{1} \\ 10.712(4) \\ 13.939(4) \\ 17.871(7) \\ 67.156(14) \\ 84.40(2) \\ 85.273(16) \\ 2444.5(17) \\ 2 \\ 1.491 \\ 0.710 \ 73 \\ 1108 \\ \text{whole data hemisphere} \\ 3-47 \\ \pm 11,\pm 15,19 \\ 7.78 \\ 0.3 \times 0.3 \times 0.4 \\ 298 \\ 9549 \\ 6877 \\ 5837 \ (>4\sigma) \\ 0.055, \ 0.068 \\ 1.89 \\ \text{SHELXTL-PLUS} \\ 556 \\ [\sigma^2(F_0) + 0.0004F_0^2]^{-1} \\ \end{array}$ | 0.40 -0.41 Con 14 C ₅₉ H ₄₈ Cl ₂ F ₁₂ N ₁₂ O ₈ P ₂ Ru ₄ 1818.21 orange, equant Siemens SMART-CCD triclinic, $P\bar{1}$ 14.4764(2) 15.0429(2) 17.0034(1) 97.829(1) 106.942(1) 103.125(1) 3367.16(7) 2 1.793 0.710 73 1796 whole data hemisphere 3-51 \pm 17, \pm 17, \pm 17,20 11.02 0.48 × 0.45 × 0.38 296 19 376 11 036 11033 (>2 σ) 0.040, 0.051 1.09 SHELXTL-PLUS 893 $[\sigma^2(F_0) + 0.0014F_0^2]^{-1}$ | 0.44 -0.36 npd 15 $C_{34}H_{25}Cl_{2}F_{6}N_{2}O_{4}PRu_{2}$ 999.6 yellow-brown, lamellar Siemens SMART-CCD orthorhombic, <i>Pbca</i> 17.614(2) 13.624(2) 31.294(2) 90 90 90 7509.6(15) 8 1.768 0.710 73 3952 whole data hemisphere 3-53 20,16,36 10.66 0.61 \times 0.46 \times 0.08 296 32 873 6756 4934 (\times 3 σ) 0.047, 0.051 1.34 SHELXTL-PLUS 497 [$\sigma^{2}(F_{0})$ + 0.00014 F_{0}^{2}] ⁻¹ | 0.42 -0.44 16 C _{47.5} H ₃₆ Cl ₃ I ₄ N ₄ O ₄ P ₂ Ru 1604.8 orange-brown, irregula Siemens P4 triclinic, PI 11.744(1) 13.357(1) 20.173(2) 93.19(1) 95.09(1) 112.90(1) 2889.3(4) 2 1.845 0.710 73 1524 25, 24 < 2 θ < 25 θ - ω 4-45 12, \pm 14, \pm 21 28.96 0.15 × 0.3 × 0.4 298 7994 7546 4260 (>6 σ) 0.048, 0.057 1.61 SHELXTL-PLUS 429 [$\sigma^2(F_0)$ + 0.0002 F_0^2]-1 | |
| $(\Delta \rho)_{\text{max}}$, e Å ⁻³ $(\Delta \rho)_{\text{min}}$, eÅ ⁻³ $(\Delta \rho)_{\text{min}}$, | $\begin{array}{c} 0.79 \\ -1.28 \\ \hline \\ \hline 12 \\ \hline \\ C_{52}H_{41}BCl_2N_6O_4Ru_2 \\ 1097.8 \\ orange, rhombohedron \\ Siemens SMART-CCD \\ triclinic, $P\overline{1}$ \\ 10.712(4) \\ 13.939(4) \\ 17.871(7) \\ 67.156(14) \\ 84.40(2) \\ 85.273(16) \\ 2444.5(17) \\ 2 \\ 1.491 \\ 0.710 \ 73 \\ 1108 \\ \text{whole data hemisphere } \\ 3-47 \\ \pm 11,\pm 15,19 \\ 7.78 \\ 0.3 \times 0.3 \times 0.4 \\ 298 \\ 9549 \\ 6877 \\ 5837 \ (>4\sigma) \\ 0.055, \ 0.068 \\ 1.89 \\ SHELXTL-PLUS \\ 556 \\ [\sigma^2(F_0) + 0.0004F_0^2]^{-1} \\ 0 \\ \end{array}$ | 0.40 -0.41 Con 14 C ₅₉ H ₄₈ Cl ₂ F ₁₂ N ₁₂ O ₈ P ₂ Ru ₄ 1818.21 orange, equant Siemens SMART-CCD triclinic, $P\bar{1}$ 14.4764(2) 15.0429(2) 17.0034(1) 97.829(1) 106.942(1) 103.125(1) 3367.16(7) 2 1.793 0.710 73 1796 whole data hemisphere 3-51 \pm 17, \pm 17, \pm 17,20 11.02 0.48 × 0.45 × 0.38 296 19 376 11 036 11033 (>2 σ) 0.040, 0.051 1.09 SHELXTL-PLUS 893 [$\sigma^2(F_0)$ + 0.0014 F_0^2] ⁻¹ 0.0024(2) | 0.44 -0.36 Inpd I5 C ₃₄ H ₂₅ Cl ₂ F ₆ N ₂ O ₄ PRu ₂ 999.6 yellow-brown, lamellar Siemens SMART-CCD orthorhombic, <i>Pbca</i> 17.614(2) 13.624(2) 31.294(2) 90 90 90 7509.6(15) 8 1.768 0.710 73 3952 whole data hemisphere 3-53 20,16,36 10.66 0.61 × 0.46 × 0.08 296 32 873 6756 4934 (>3 σ) 0.047, 0.051 1.34 SHELXTL-PLUS 497 $[\sigma^2(F_0) + 0.00014F_0^2]^{-1}$ 0.00027(3) | 0.42 -0.44 16 C _{47.5} H ₃₆ Cl ₃ I ₄ N ₄ O ₄ P ₂ R ₁ 1604.8 orange-brown, irregulation of the control of th | |
| $(\Delta \rho)_{\text{max}}$, e Å ⁻³ $(\Delta \rho)_{\text{min}}$, eÅ ⁻³ $(\Delta \rho)_{\text{min}}$, | $\begin{array}{c} 0.79 \\ -1.28 \\ \hline \\ \textbf{12} \\ \hline \\ \textbf{C}_{52}H_{41}BCl_2N_6O_4Ru_2 \\ 1097.8 \\ \text{orange, rhombohedron} \\ \text{Siemens SMART-CCD} \\ \text{triclinic, } P\overline{1} \\ 10.712(4) \\ 13.939(4) \\ 17.871(7) \\ 67.156(14) \\ 84.40(2) \\ 85.273(16) \\ 2444.5(17) \\ 2 \\ 1.491 \\ 0.710 \ 73 \\ 1108 \\ \text{whole data hemisphere} \\ 3-47 \\ \pm 11,\pm 15,19 \\ 7.78 \\ 0.3 \times 0.3 \times 0.4 \\ 298 \\ 9549 \\ 6877 \\ 5837 \ (>4\sigma) \\ 0.055, \ 0.068 \\ 1.89 \\ \text{SHELXTL-PLUS} \\ 556 \\ [\sigma^2(F_0) + 0.0004F_0^2]^{-1} \\ \end{array}$ | 0.40 -0.41 Con 14 C ₅₉ H ₄₈ Cl ₂ F ₁₂ N ₁₂ O ₈ P ₂ Ru ₄ 1818.21 orange, equant Siemens SMART-CCD triclinic, $P\bar{1}$ 14.4764(2) 15.0429(2) 17.0034(1) 97.829(1) 106.942(1) 103.125(1) 3367.16(7) 2 1.793 0.710 73 1796 whole data hemisphere 3-51 \pm 17, \pm 17, \pm 17,20 11.02 0.48 × 0.45 × 0.38 296 19 376 11 036 11033 (>2 σ) 0.040, 0.051 1.09 SHELXTL-PLUS 893 $[\sigma^2(F_0) + 0.0014F_0^2]^{-1}$ | 0.44 -0.36 npd 15 $C_{34}H_{25}Cl_{2}F_{6}N_{2}O_{4}PRu_{2}$ 999.6 yellow-brown, lamellar Siemens SMART-CCD orthorhombic, <i>Pbca</i> 17.614(2) 13.624(2) 31.294(2) 90 90 90 7509.6(15) 8 1.768 0.710 73 3952 whole data hemisphere 3-53 20,16,36 10.66 0.61 \times 0.46 \times 0.08 296 32 873 6756 4934 (\times 3 σ) 0.047, 0.051 1.34 SHELXTL-PLUS 497 [$\sigma^{2}(F_{0})$ + 0.00014 F_{0}^{2}] ⁻¹ | 0.42 -0.44 16 C _{47.5} H ₃₆ Cl ₃ I ₄ N ₄ O ₄ P ₂ Ru 1604.8 orange-brown, irregulated Siemens P4 triclinic, PI 11.744(1) 13.357(1) 20.173(2) 93.19(1) 95.09(1) 112.90(1) 2889.3(4) 2 1.845 0.710 73 1524 25, 24 < 2 θ < 25 θ - ω 4-45 12, \pm 14, \pm 21 28.96 0.15 × 0.3 × 0.4 298 7994 7546 4260 (>6 σ) 0.048, 0.057 1.61 SHELXTL-PLUS 429 [$\sigma^2(F_0)$ + 0.0002 F_0^2]-1 | |

 $^{^{}a}R = [\Sigma ||F_{\rm o}| - |F_{\rm c}||/\Sigma |F_{\rm o}]. \ \ R_{\rm w} = [\Sigma w(|F_{\rm o}| - |F_{\rm c}|)^{2}/\Sigma w|F_{\rm o}|^{2}]^{1/2}. \ \ {\rm GOF} = [\Sigma w(|F_{\rm o}| - |F_{\rm c}|)^{2}/(N_{\rm o} - N_{\rm p})]^{1/2}.$

molecule of CH₂Cl₂, which was later confirmed by the elementary analysis results and the ¹H NMR spectral evidence. Yield: 63%. Anal. Calcd for $C_{63}H_{58}Cl_2N_4O_2P_4Ru_2$: C, 58.11; H, 4.64; N, 4.30. Found: C, 58.14; H, 4.67; N, 4.40. ¹H NMR (25 °C, 200 MHz, CDCl₃): dppm at 7.71-6.99 (m, 40 H), 4.95 (m, 4 H); H⁴ on μ -Pz' at 5.44 (br, 2 H); Me³ and Me⁵ on μ -Pz'

at 2.10 (s, 6 H), 1.15 (s, 6 H). ³¹P{¹H} NMR (25 °C, 162 MHz, CDCl₃): 11.41 (m, 2 P), -30.26 (m, 2 P). IR (CH₂Cl₂): v_{CO} , 1914 s, 1892 s cm⁻¹.

Reaction between 1-3 and N-N (N-N = bpy, phen). A typical reaction is shown as follows. In a 100-mL Schlenk flask was added 1 (205 mg, 0.350 mmol), bpy (116 mg, 0.742 mmol), and 25 mL of MeOH at room temperature. The mixture was then heated under reflux for 5 h and then cooled to room temperature. A 252 mg amount of NaBPh4 (0.732 mmol) dissolving in 10 mL of Me $\bar{C}N$ was added to the mixture, forming a precipitate within 30 min. The solvents were removed under vacuum. Recrystallization from CH2Cl2/MeOH gave crude product, which was then washed three times each with 5 mL of MeOH and 5 mL of Et₂O to remove completely the unreacted bpy and dried in vacuo to give 207 mg of pure $[Ru_2(\mu-Pz)(\mu-CO)_2(CO)_2(\mu_1,\eta^2-bpy)_2][BPh_4]$ (12) (58%). Anal. Calcd for C₅₁H₃₉BN₆O₄Ru₂: C, 60.47; H, 3.88; N, 8.29. Found: C, 60.27; H, 3.78; N, 8.14. ¹H NMR (25 °C, 200 MHz, acetone-d₆): bpy at 10.16 (m, 4 H), 8.92 (m, 4 H), 8.50 (m, 4 H), 8.14 (m, 4 H); BPh₄ at 7.35 (m, 8 H), 6.87 (m, 8 H), 6.75 (m, 4 H); H³ and H⁵ on μ -Pz at 5.80 (d, 2 H, J = 2.2); H⁴ on μ -Pz at 5.29 (t, 1 H). IR (CH₂Cl₂): v_{CO} , 2028 s, 1994 w, 1801 w, 1746 s cm⁻¹. A similar reaction between 1 and phen gave $[Ru_2(\mu-Pz)(\mu-CO)_2(CO)_2(\mu_1,\eta^2-phen)_2][BPh_4]$ (13) (68%). Anal. Calcd for $C_{55}H_{39}BN_6O_4Ru_2$: C, 62.26; H, 3.71; N, 7.92. Eound: C, 62.03; H, 3.46; N, 8.02. ¹H NMR (25 °C, 200 MHz, Exertone- d_6): phen at 10.50 (dd, 4 H, J = 1.4, 5.2), 9.11 (dd, 4 $\hat{\mathbf{B}}$, J = 1.4, 8.2), 8.49 (dd, 4 H, J = 5.2, 8.2), 8.46 (s, 4 H); BPh₄ at 7.34 (m, 8 H), 6.92 (m, 8 H), 6.75 (m, 4 H); H³ and H⁵ on $\not E$ Pz at 5.34 (d, 2 H, J = 2.0); H⁴ on μ -Pz at 5.06 (t, 1 H). IR $E_{\rm C}^{\rm H_2Cl_2}$: $\nu_{\rm CO}$, 2028 s, 1994 w, 1801 w, 1746 s cm⁻¹. Following procedure similar to that for 12, the reaction of 2 and 3 with bpy in the presence of NaPF₆ gave only one identical product $[\Re u_2(\mu-Pz')(\mu-CO)_2(CO)_2(\mu_1,\eta^2-bpy)_2][PF_6]$ (14) in 73 and 85% geld, respectively. Anal. Calcd for C29H23F6N6O4PRu2: C, 40.19; H, 2.67; N, 9.69. Found: C, 39.88; H, 2.81; N, 9.80. ¹H MR (25 °C, 200 MHz, CDCl₃): bpy at 10.24 (m, 4 H), 8.67 \succeq $(E, 200 \text{ MHz}, CDC_{13})$. bpy at 10.24 (iii, 4 H), 8.07 (E, 4 H), 8.38 (m, 4 H), 7.95 (m, 4 H); H⁴ on μ -Pz' at 4.84 (s, E, 4 H); Me³ and Me⁵ on μ -Pz' at 3.50 (br, 6 H). IR (CH₂Cl₂): \mathbb{R}^{17} , \mathbb{R}^{18} the third like on μ 12 at 0.00 (b), \mathbb{R}^{18} . It (\mathbb{R}^{18}) is \mathbb{R}^{18} , \mathbb{R}^{18} , \mathbb{R}^{18} , \mathbb{R}^{18} , \mathbb{R}^{18} and \mathbb{R}^{18} in the presence of \mathbb{R}^{18} gave only one identical product \mathbb{R}^{18} (\mathbb{R}^{18}) in \mathbb{R}^{18} and \mathbb{R}^{18} (\mathbb{R}^{18}) in \mathbb{R}^{18} in $\mathbb{R}^{$ Field, respectively. Anal. Calcd for C₃₃H₂₃F₆N₆O₄PRu₂: C, 43.33; H, 2.53; N, 9.18. Found: C, 43.28; H, 2.60; N, 9.37. ¹H $\overline{\mathbf{N}}$ MR (25 °C, 200 MHz, CDCl₃): phen at 10.65 (d, 4 H, J =52), 9.20 (d, 4 H, J = 8.2), 8.62 (dd, 4 H, J = 5.2, 8.2), 8.54 (s, 4 H); H⁴ on μ -Pz' at 4.78 (s, 1 H); Me³ and Me⁵ on μ -Pz' at 2.81 (\$, 6 H). IR (CH₂Cl₂): v_{CO} , 2026 s, 1991 w, 1801 w, 1744 s

Reaction between Et₃O+BF₄- and 1-3. A typical reaction is shown as follows. To the solution of 1, prepared by dissolving 1 (100 mg, 0.171 mmol) in 1 mL of MeCN and 10 mL of CH₂Cl₂ in a 100-mL Schlenk flask, was added with 1 mL of Et₃O⁺BF₄⁻ solution (1 M in CH₂Cl₂). The mixture was then stirred for 1 h at room temperature, giving a solution IR spectrum with three typical carbonyl stretching bands at 2062 m, 2033 s, and 1993 s cm⁻¹ for [Ru₂(CO)₄(MeCN)₆][BF₄]₂,⁴ which can be converted into [Ru₂(CO)₄(MeCN)₄(PPh₃)₂][BF₄]₂ by following the established procedure. 4a Yield: 90%.

Reaction between Et₃O⁺BF₄⁻ and 4-6. A typical reaction is shown as follows. To the solution of 4, prepared by dissolving 5 (100 mg, 0.101 mmol) in 10 mL of CH₂Cl₂ and 1 mL of MeCN in a 100-mL Schlenk flask, was added with 0.5 mL of Et₃O⁺BF₄⁻ solution (1 M in CH₂Cl₂). The mixture was then stirred for 2 h at room temperature, and 5 mL of MeOH was added to decompose unreacted Et₃O⁺BF₄⁻. Volatile substance was removed under vacuum. Recrystallization from CH₂Cl₂/MeOH gave 105 mg of pure solid. It was identified as [Ru₂(CO)₄(MeCN)₄(PPh₃)₂][BF₄]₂ by comparing the spectral evidences with those reported.4 Yield: 88%.

Reaction between 4 and I2. In a 100-mL Schlenk flask was added 4 (107 mg, 0.110 mmol) and 5 mL of CH₂Cl₂ at room temperature. This solution was then added dropwise with a CH₂Cl₂ solution of I₂, prepared by dissolving 2 equiv of I₂ (ca. 0.060 g) in 5 mL of CH₂Cl₂. The mixture was stirred for 0.5 h, and the solvent was then removed under vacuum. Recrystallization from CH2Cl2/MeOH afforded 0.108 g of the pure product $[Ru_2(\mu-Pz)_2(\mu-I)(CO)_4(PPh_3)_2][I_3]$ (16) in 73% yield. Anal. Calcd for C₄₆H₃₆I₄N₄O₄P₂Ru₂: C, 37.32; H, 2.45; N, 3.78. Found: C, 37.56; H, 2.54; N, 3.92. ¹H NMR (25 °C, 200 MHz, acetone- d_6): PPh₃ at 7.79–7.53 (m, 30 H); H³ and H⁵ on μ -Pz at 6.99 (d, 4 H, J = 2.3); H⁴ on μ -Pz at 5.74 (t, 2 H). 31 P{ 1 H} NMR (25 °C, 162 MHz, acetone- d_6): 38.74 (s, 2 P). IR: v_{CO} , 2072 s, 2024 s cm⁻¹ in CH₂Cl₂; v_{CO} , 2068 s, 2016 s cm⁻¹ in KBr.

Single-Crystal X-ray Diffraction Studies of 2, 5, 10-**12, and 14–16.** Suitable single crystals were grown from CH₂-Cl₂/hexane or CH₂Cl₂/Et₂O at room temperature to do the single-crystal structure determination. The X-ray diffraction data for 2, 5, 10, and 16 were measured on a four-circle diffractometer, and those for 11, 12, 14, and 15 were measured in frames with increasing ω (0.3°/frame) and with the scan speed at 10.00 s/frame on a Siemens SMART-CCD instrument, equipped with a normal focus and 3 kW sealed-tube X-ray source. For data collected on the four-circle diffractometer, three standard reflections were monitored every 1 h or every 50 reflections throughout the collection. The variation was less than 2%. Empirical absorption corrections were carried out on the basis of an azimuthal scan. For 2, the structure was solved by direct methods and refined by a full-matrix least-squares procedure using TEXSAN.8 For 5 and 10, the structures were solved by heavy-atom method and refined by a full-matrix least-squares procedure using NRCVAX.9 For 11, **12**, and **14–16**, the structures were solved by direct methods and refined by a full-matrix least-squares procedure using SHELXTL-PLUS.¹⁰ The other essential details of singlecrystal data measurement and refinement are given in Table 2. One molecule of CH₂Cl₂ was found in the asymmetric unit of the crystals used for 11, 12, and 14, whereas one and a half molecules of CH₂Cl₂ were located for 16. The solvent hydrogen positions in this structure were not included in the structure refinement.

Acknowledgment. Financial support for this work by the National Science Council of Republic of China (Contract NSC85-2113-M006-012) is gratefully acknowledged.

Supporting Information Available: An ORTEP plot for **14B** (Figure 9) and tables of non-hydrogen atomic coordinates and equivalent isotropic displacement coefficients, complete bond lengths and angles, anisotropic displacement coefficients, and hydrogen coordinates and B values for **2**, **5**, **10**–**12**, and 14-16 (58 pages). Ordering information is given on any current masthead page.

OM9600708

⁽⁸⁾ Crystal Structure Analysis Package, Molecular Structure Corp.,

The Woodlands, TX, 1985, 1992. (9) Gabe, E. J.; Le page, Y.; Charland, J.-P.; Lee, F. L.; White, P. S. Appl. Crystallogr. 1989, 22, 384.

^{(10) (}a) Sheldrick, G. M. SHELXTL-Plus Crystallographic System, release 4.21; Siemens Analytical X-ray Instruments: Madison, WI, 1991. (b) Siemens Analytical X-ray Instruments Inc., Karlsruhe, Germany, 1991.